

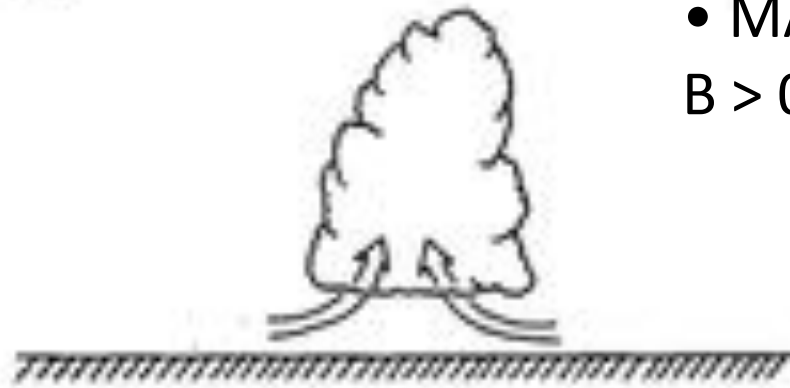


17 March 2012 © H. Bluestein

- NO VERTICAL SHEAR

- BASIC BUILDING BLOCK FOR ALL CONVECTIVE STORMS

(a)



- MAINLY UPDRAFTS

$B > 0$

(b)



- MAINLY DOWNDRAFTS

$B < 0$

FIG. 1. Schematic illustration of the life cycle of an ordinary thunderstorm cell in which the (a) initial updraft, yields to a (b) downdraft produced by the accumulation of rain within the updraft. (Adapted from Figs. 17-18 of Byers and Braham, 1949.)

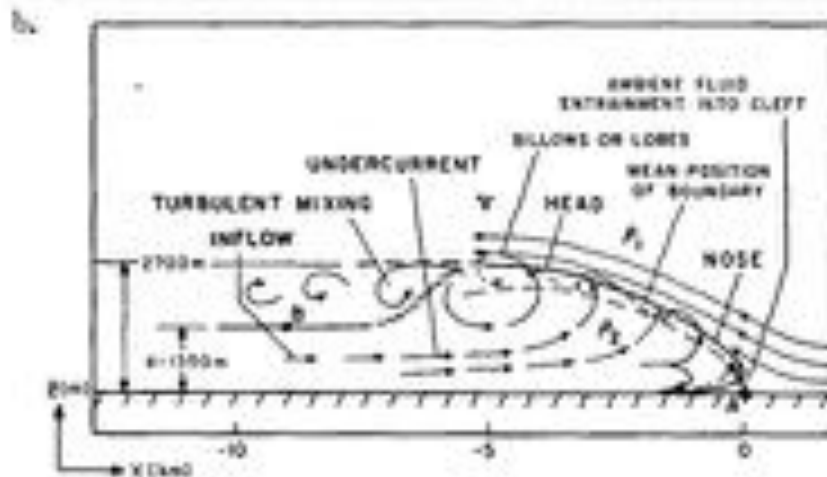
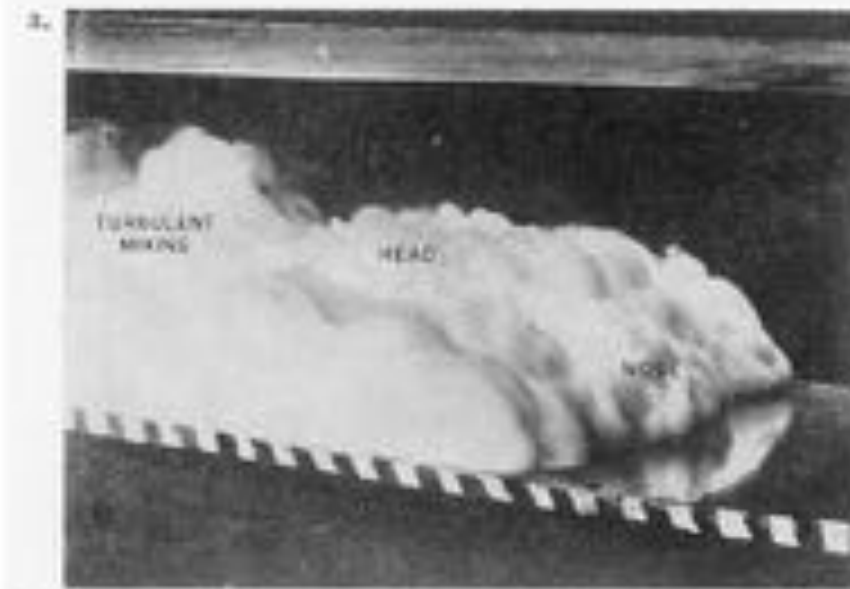
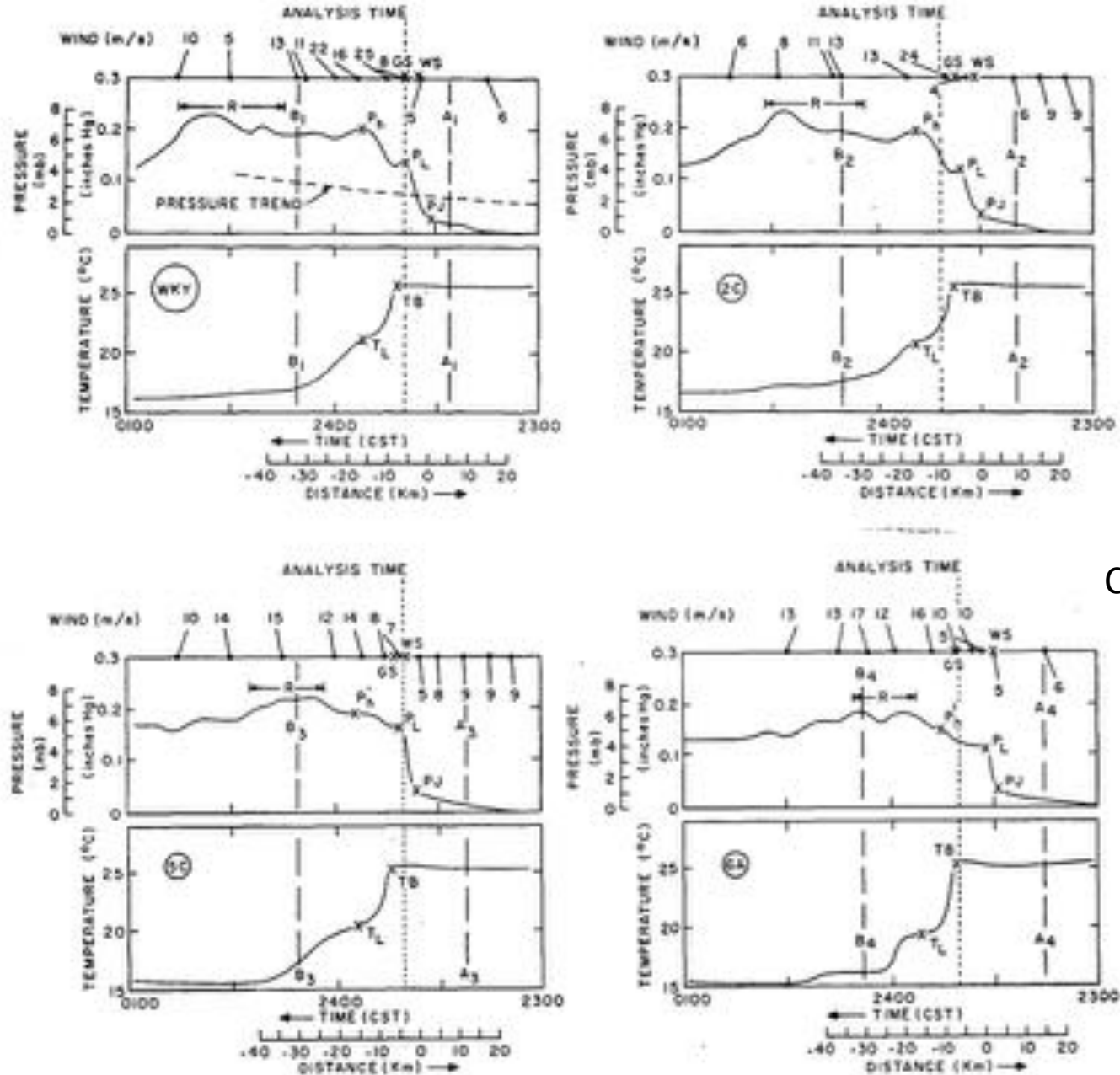


FIG. 13. (a) A gravity current (also called density current) simulated in a laboratory experiment (reproduced from Simpson, 1969). The white mass is a saline solution, flowing to the right along the bottom of a trough filled with pure water (compare with Fig. 12). (b) Schematic (laboratory) gravity current mode, (constructed from the work of Keulegan, 1958; Middleton, 1966; and Simpson, 1969; 1972). The vertical and horizontal dimensions of the model are scaled to the dimensions of the gust front.

Charba 1974



Charba 1974

FIG. 5. Time-to-space scale sections of surface wind, pressure, and temperature normal to the leading edge of the gust frontal air mass at network stations WKY, 2C, 5C, and 6A. The long-dashed vertical lines labeled A_1 and B_1 at WKY, A_2 and B_2 at 2C, etc., denote the end points of the corresponding section lines A_nB_n , A_nB_n , etc., in the network fields. The short-dashed vertical line labeled "analysis time" denotes the time of the surface network analysis (2337:30 CST). Significant points along each curve are marked and labeled; these points are located in the appropriate network fields. In all sections "R" stands for heavy rain.

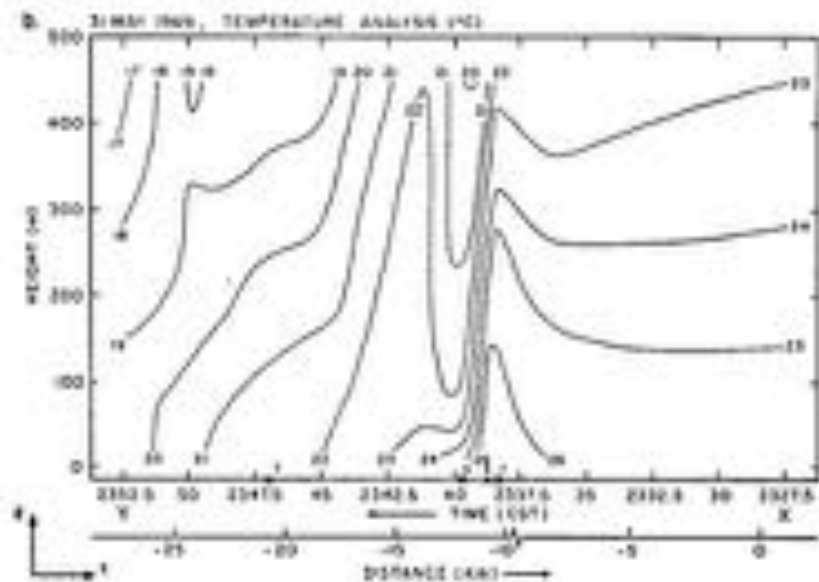
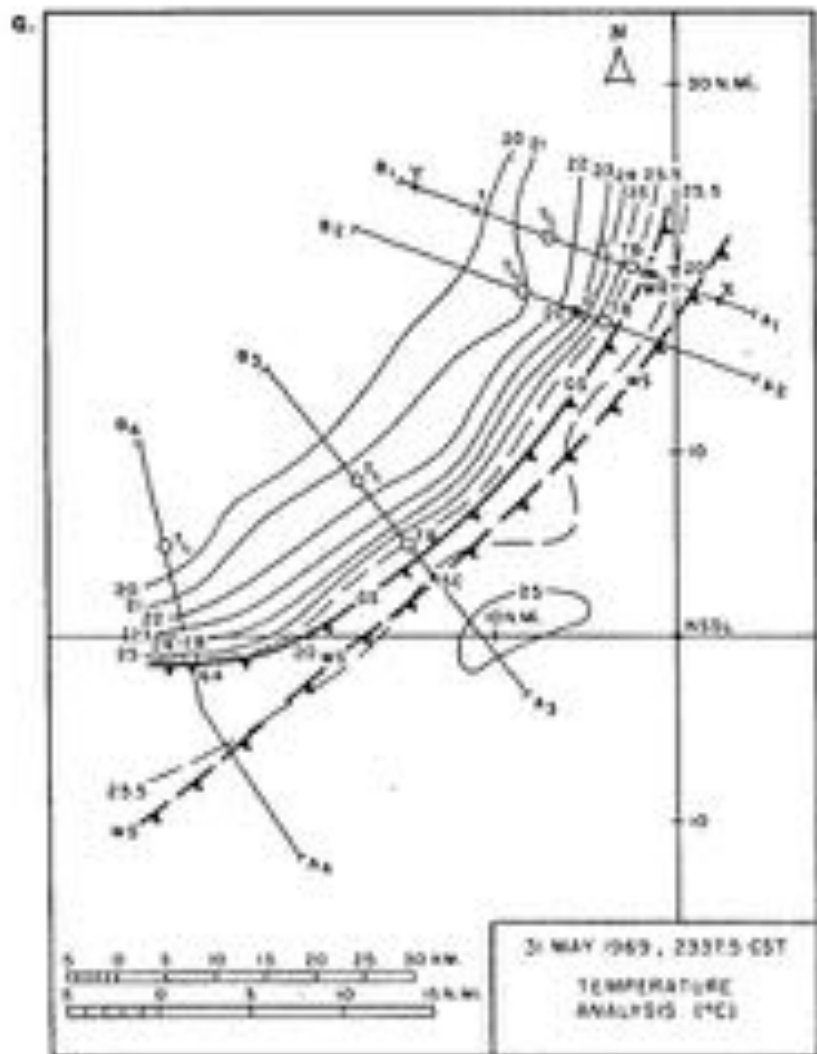
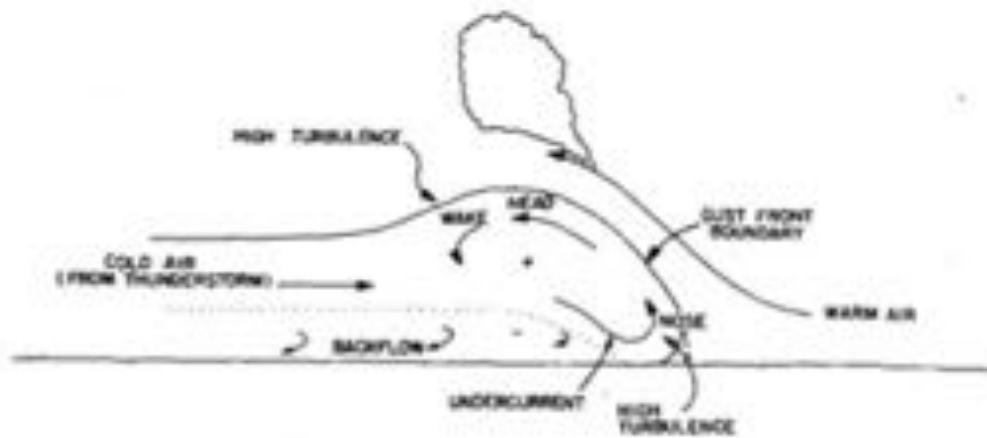


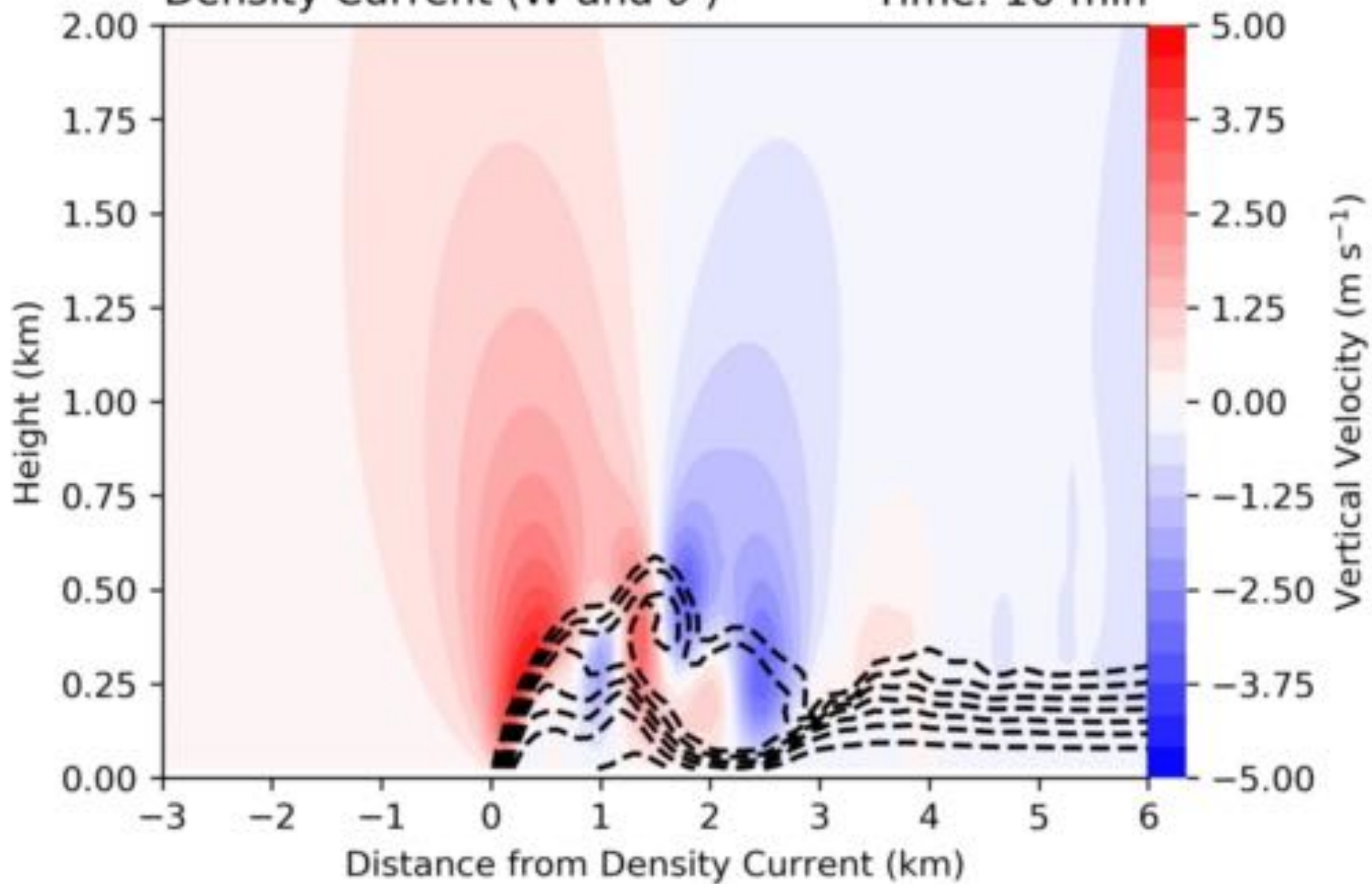
FIG. 6. Network and tower temperature analysis. Significant points along the section lines in (a) are denoted as discussed earlier (see Fig. 5).



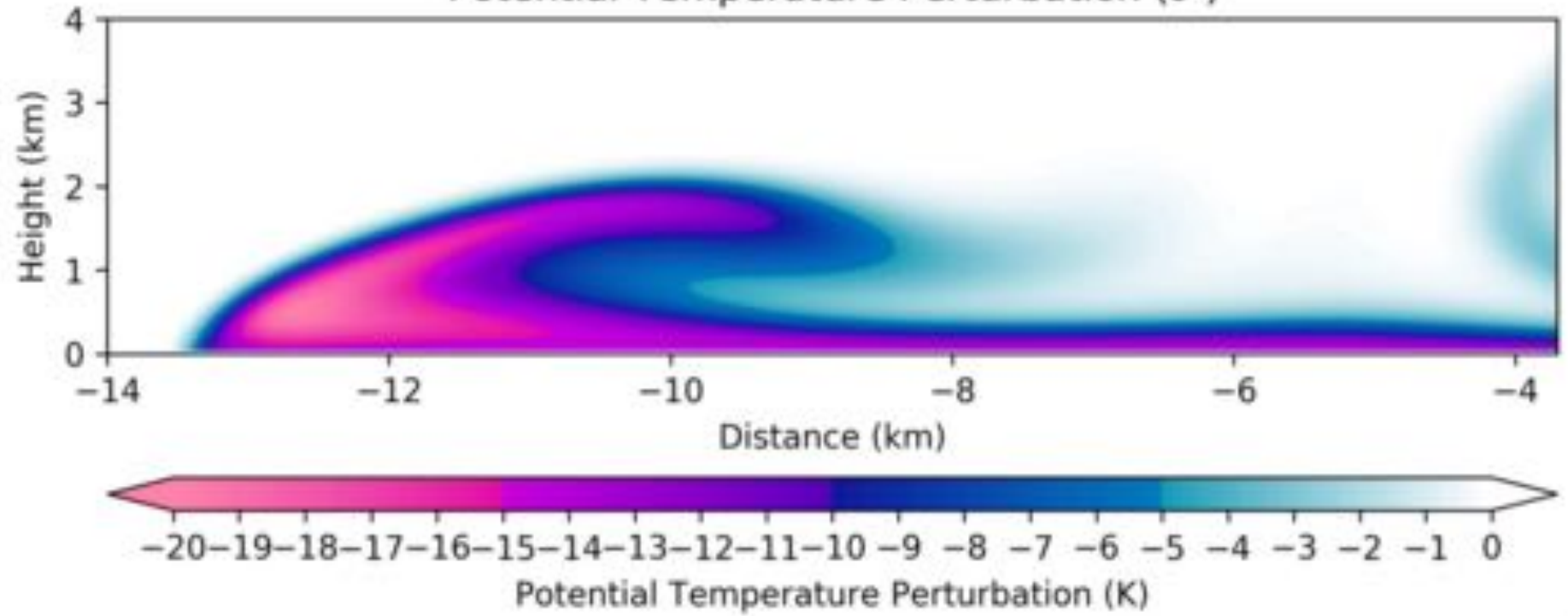
Goff 1976

Density Current (W and θ')

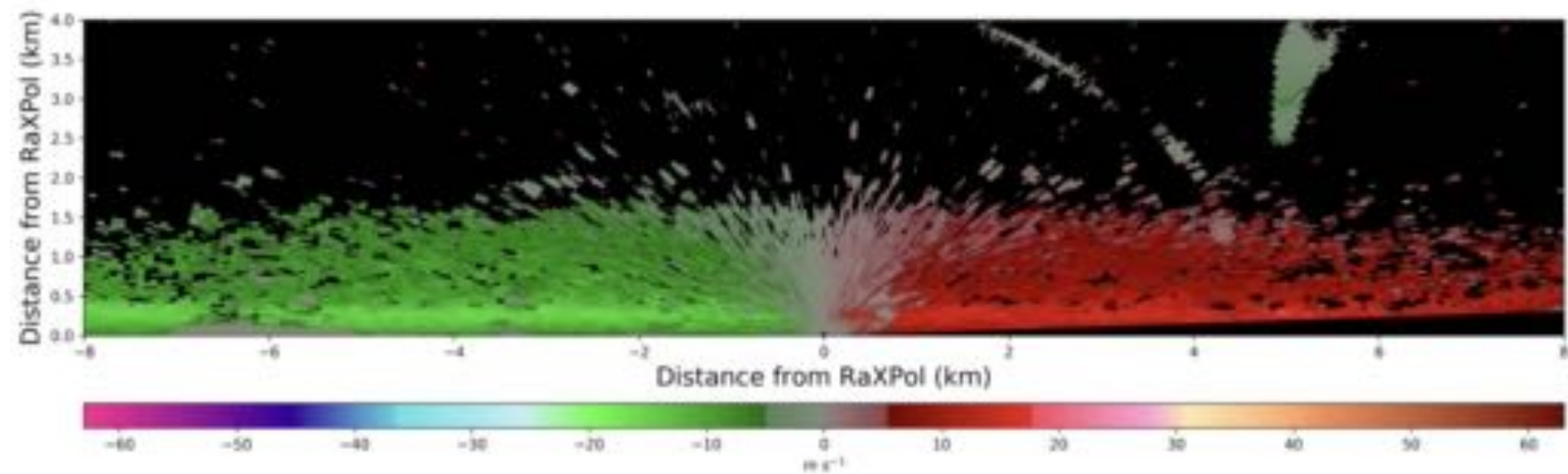
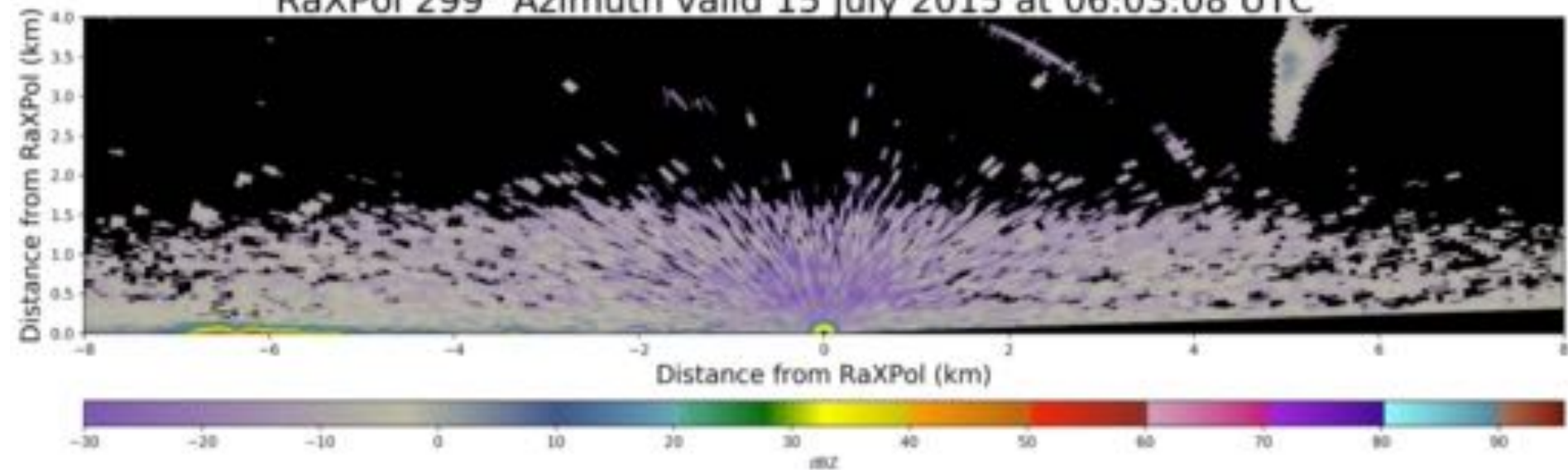
Time: 10 min



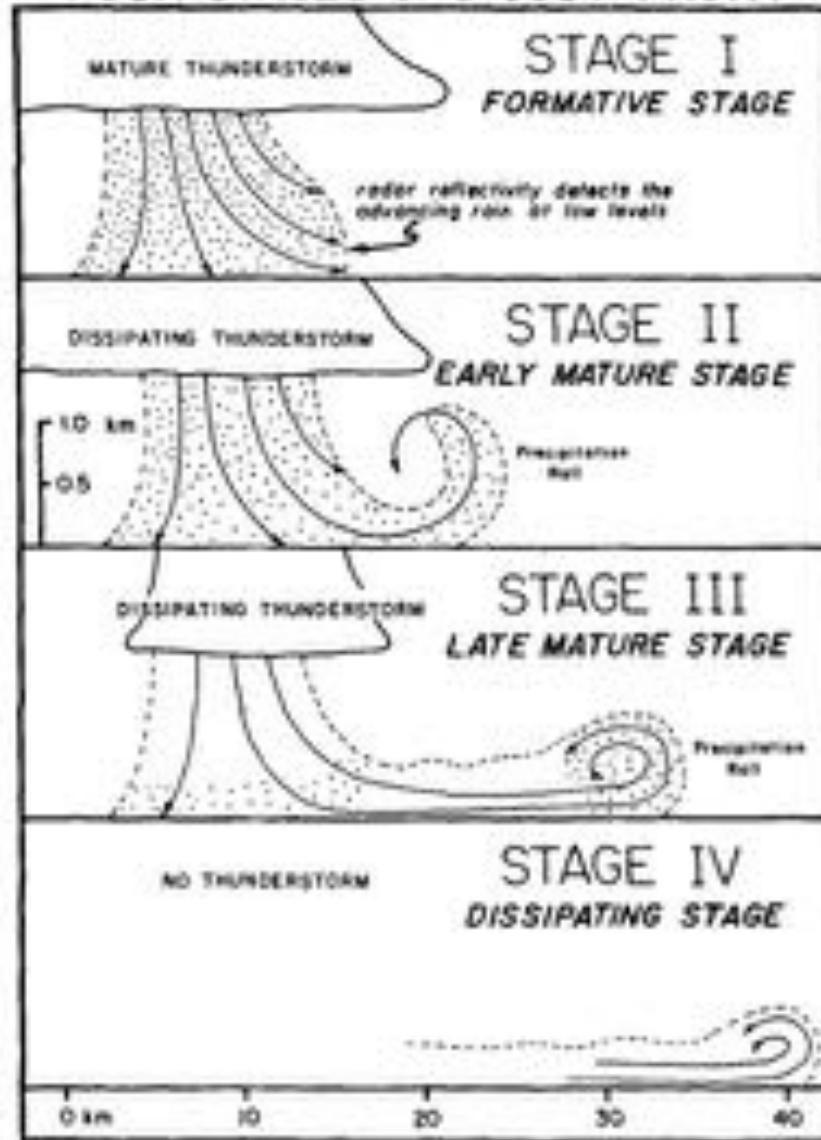
Potential Temperature Perturbation (θ')



RaXPol 299° Azimuth valid 15 July 2015 at 06:03:08 UTC



FOUR STAGES of a GUST FRONT



Wakimoto 1982

NIMROD 1978

FIG. 3. The four stages of a thunderstorm gust front. The advancing precipitation at low levels is detected by the radar. The "precipitation roll" is a horizontal roll formed by airflow that is deflected upwards by the ground.

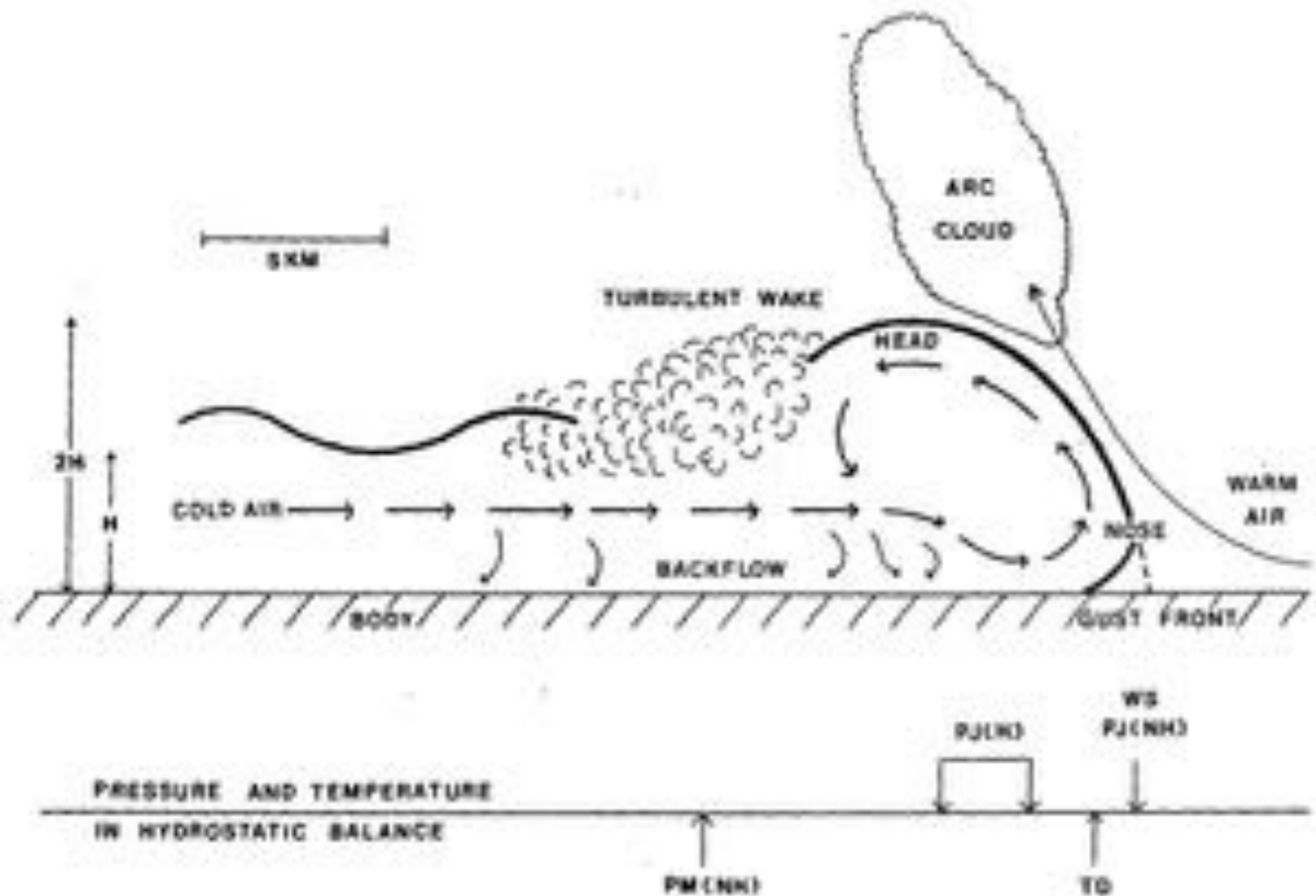
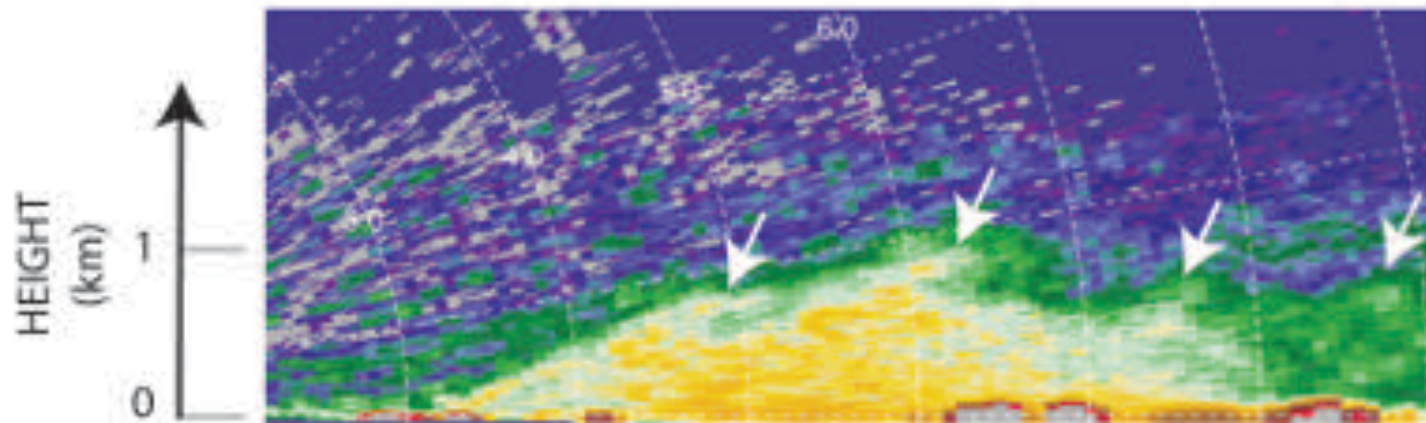
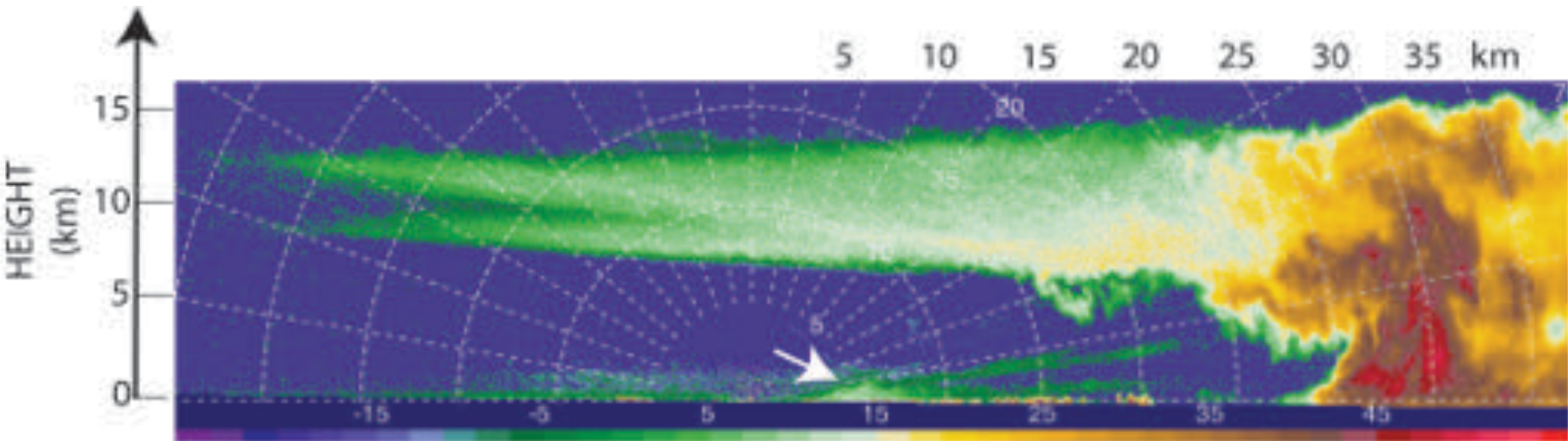
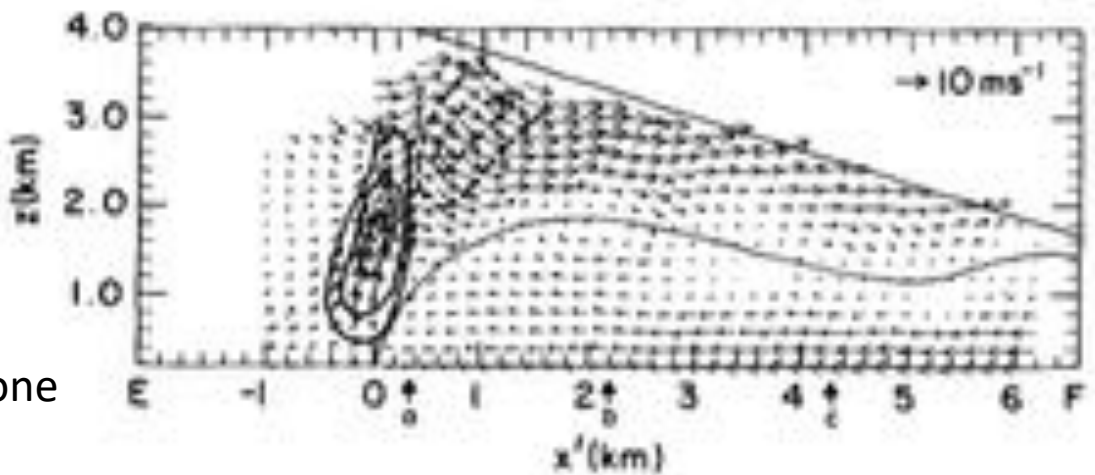
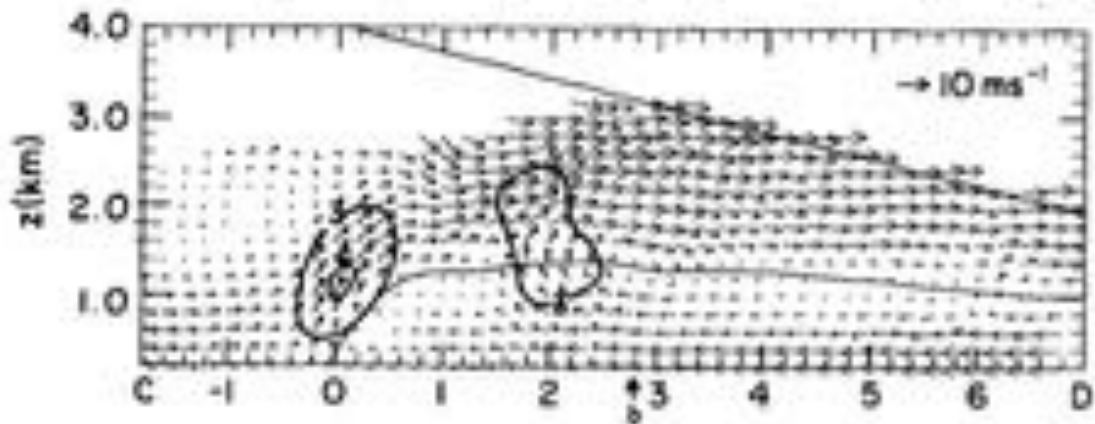
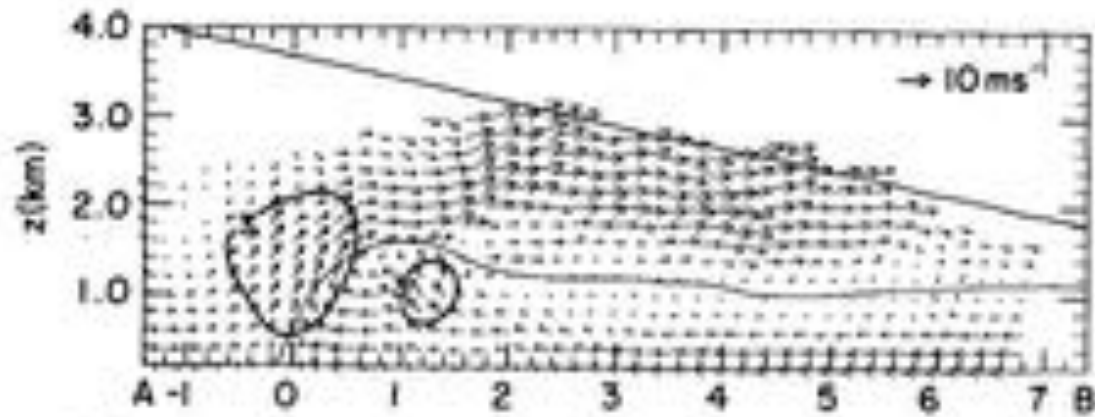


FIG. 1. Schematic vertical cross section through a mature thunderstorm outflow (vertical scale exaggerated), and the corresponding changes in surface meteorological parameters. See the text for details. (Adapted from Charba, 1974; Goff, 1975; Wakimoto, 1982; Koch, 1984).

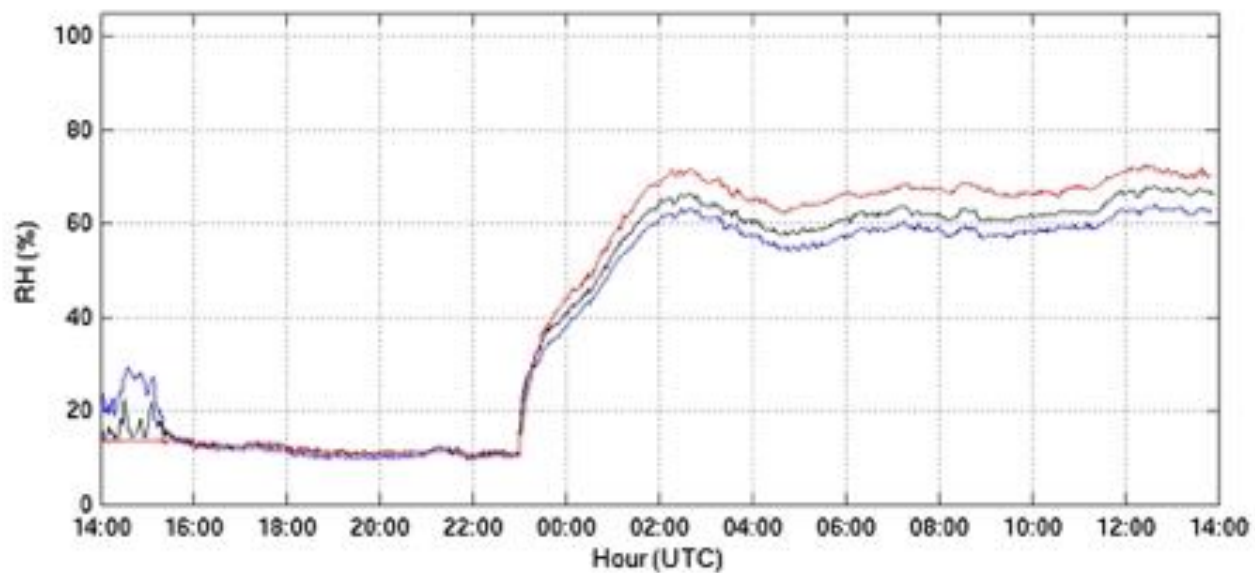
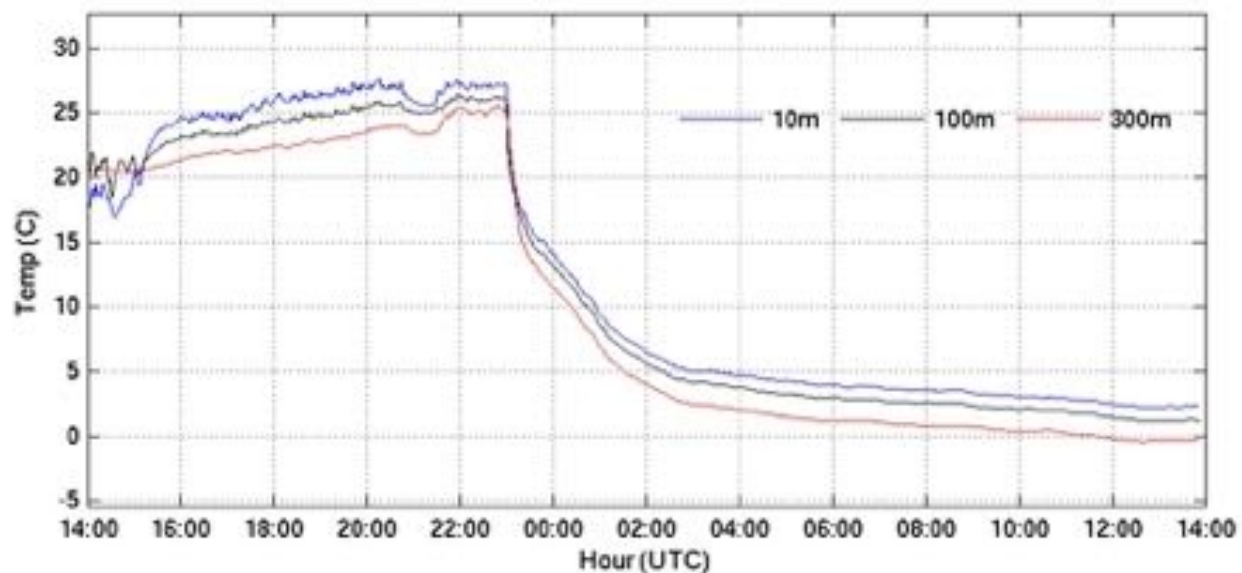


15 JULY 2015 PECAN
WESTERN KANSAS

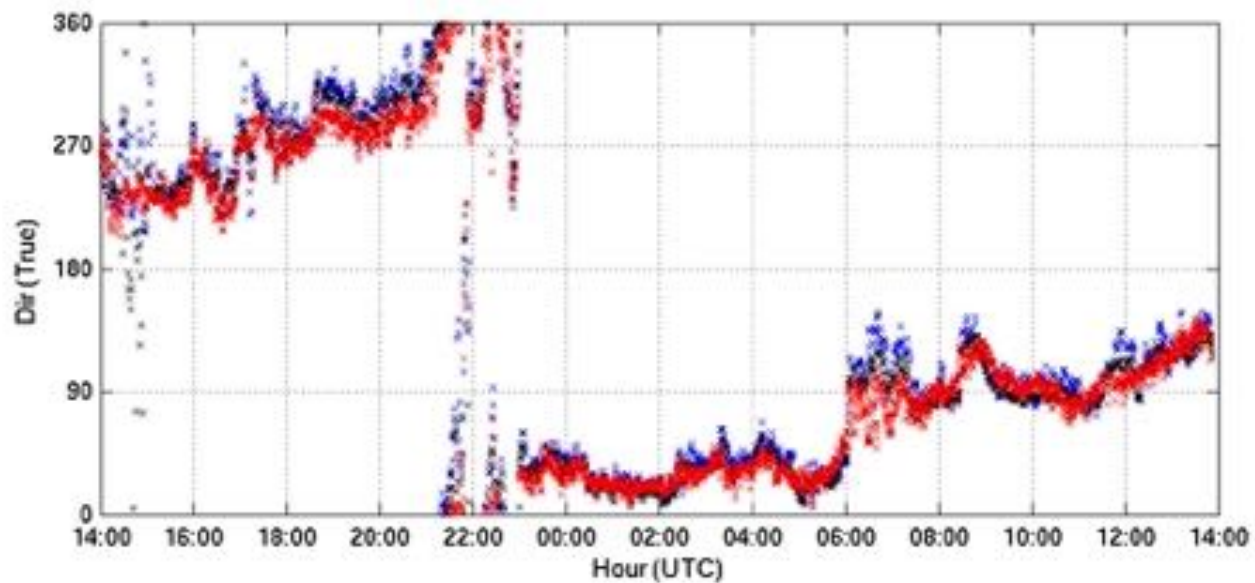
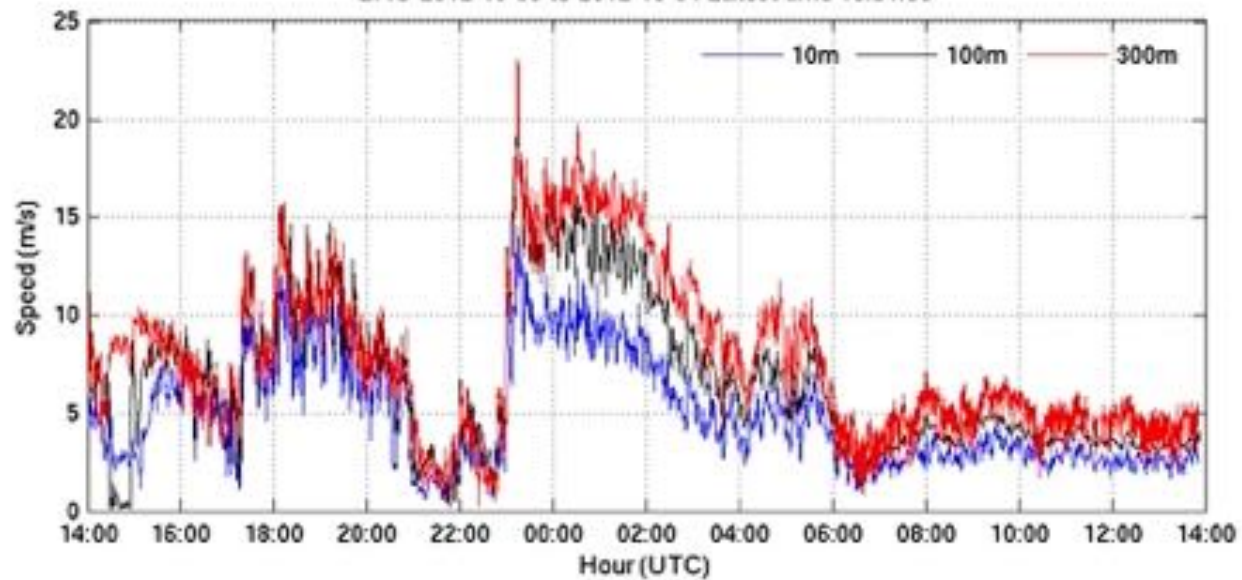


Mueller and Carbone
1987

BAO 2012-10-03 to 2012-10-04 Latest time 13:51:00



BAO 2012-10-03 to 2012-10-04 Latest time 13:51:00

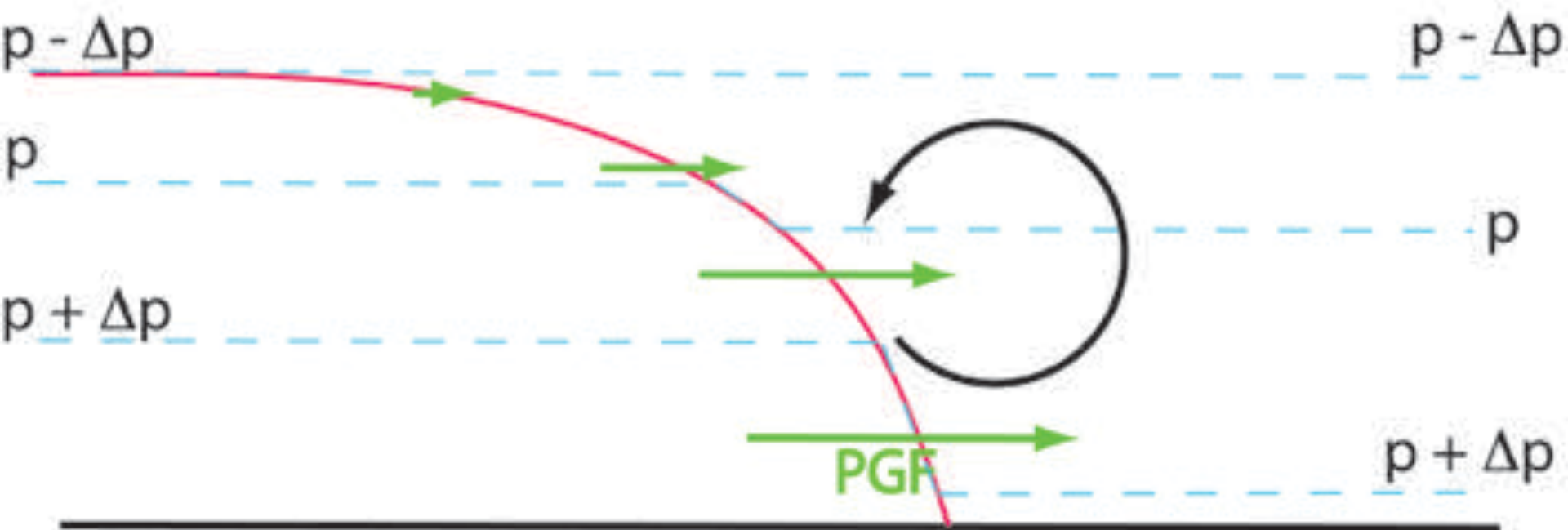


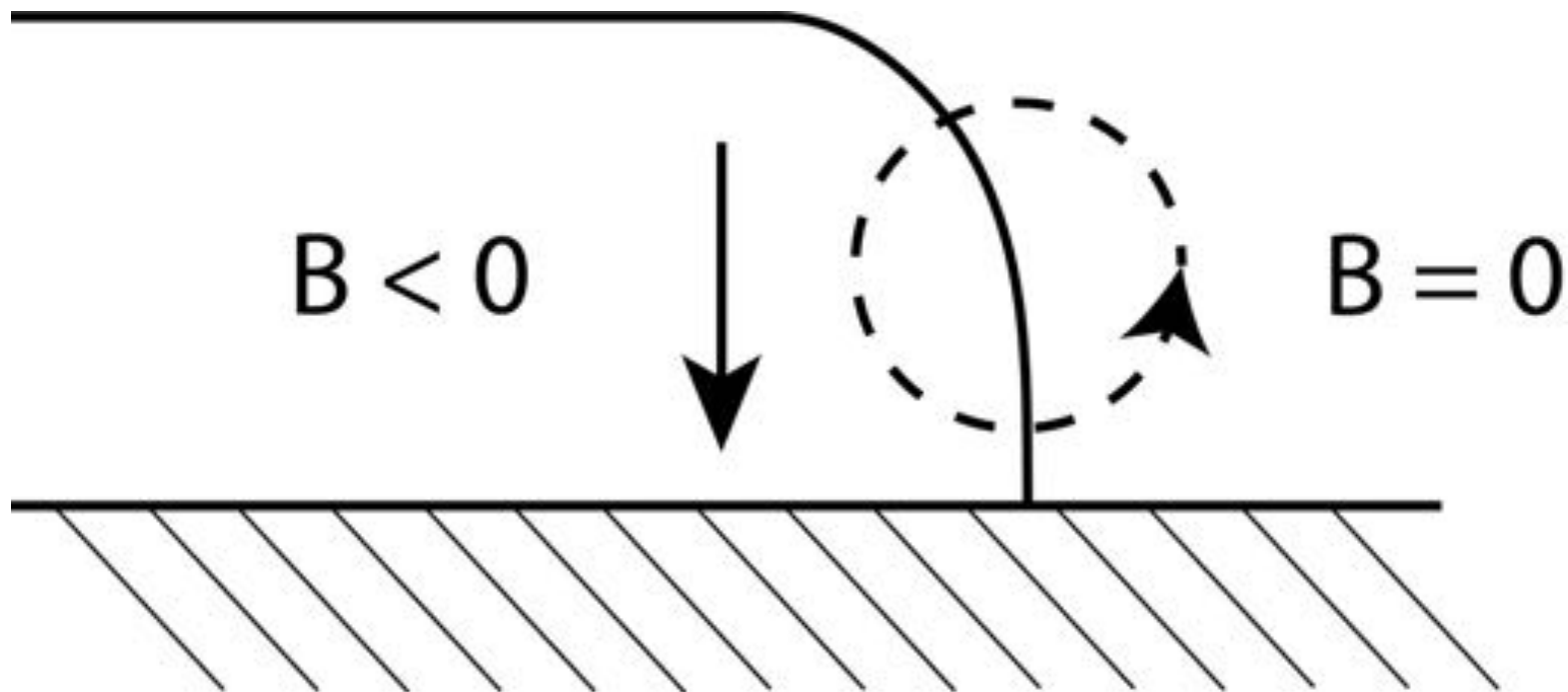


PRECIPITATION CORE

© H. Bluestein

WHALE'S MOUTH





WARM

IN GROUND-RELATIVE
REFERENCE FRAME

COLD

H



L

(a)

IN REFERENCE FRAME
OF DENSITY CURRENT

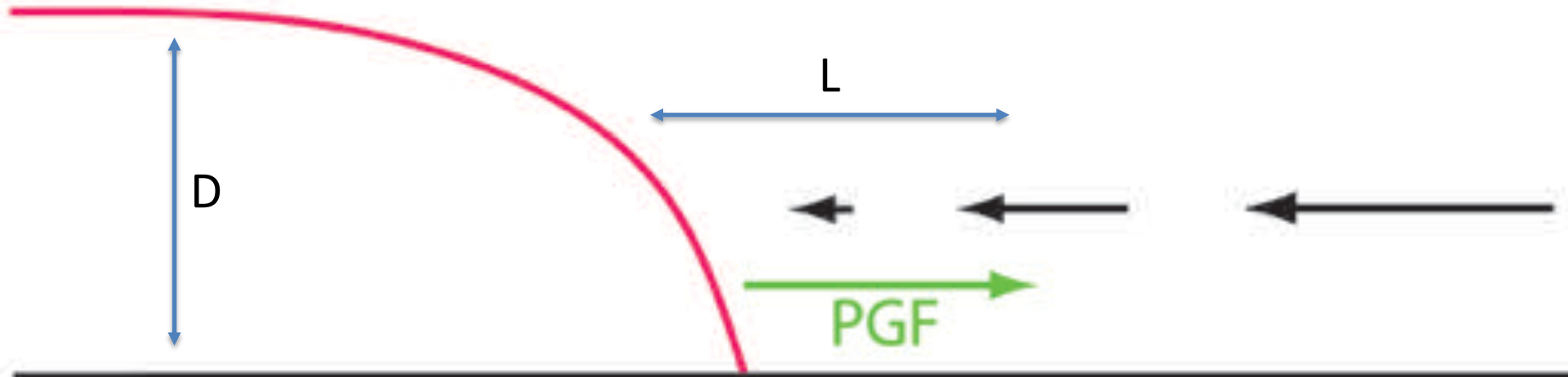


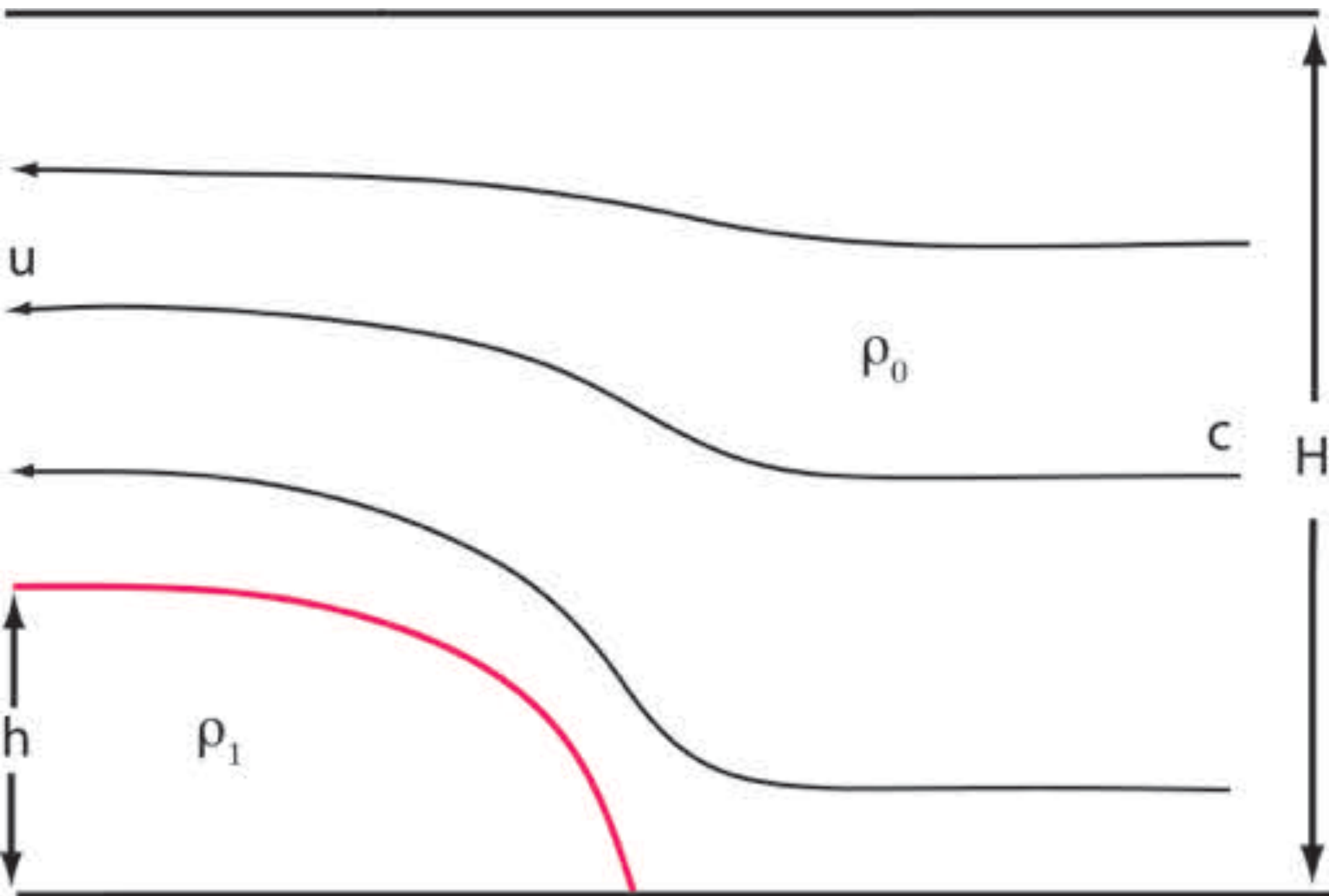
H



(b)

$$W/D \sim U/L$$
$$W \sim U, \text{ so } L \sim D$$





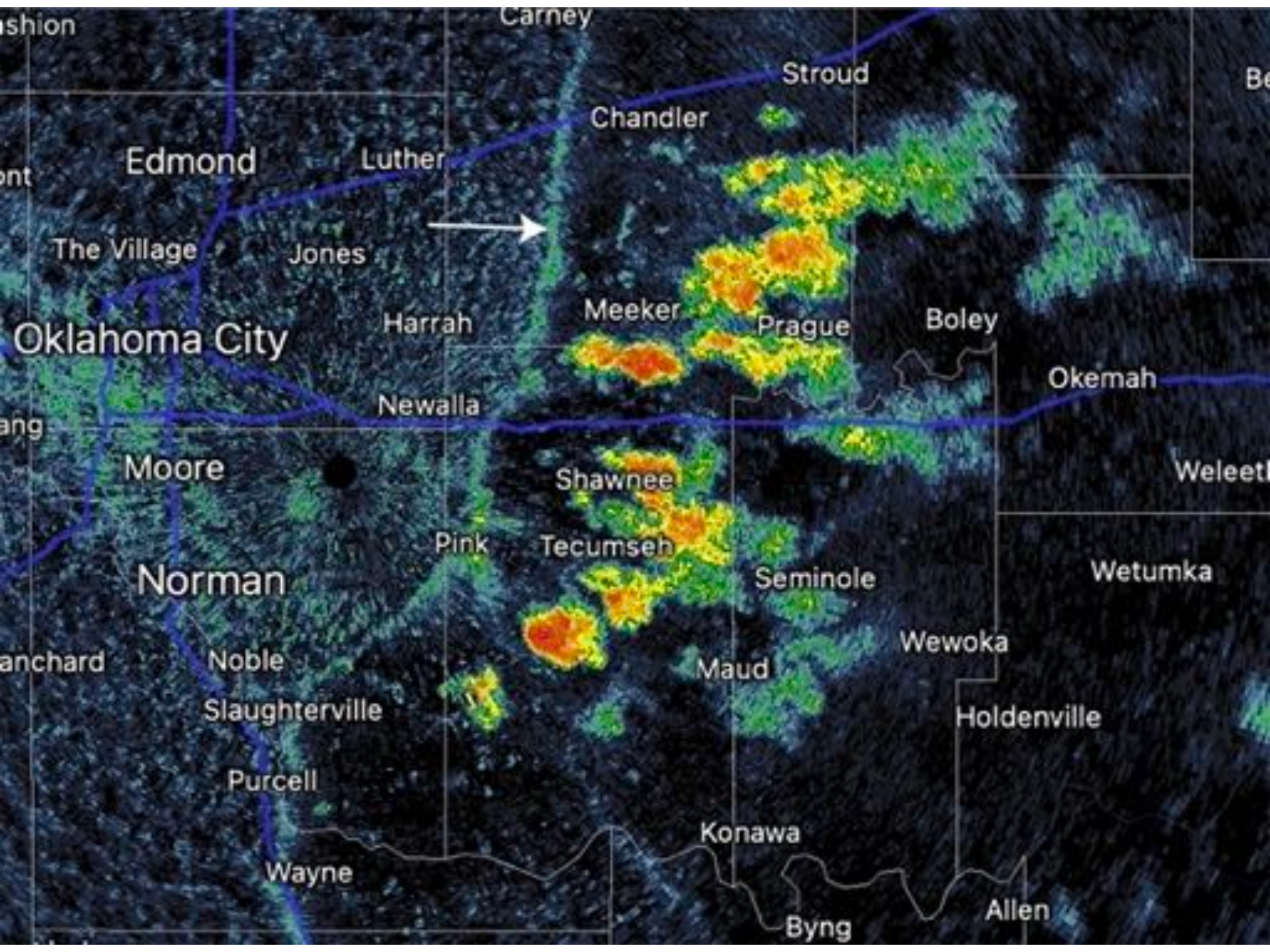


TABLE 1. List of downdraft forcing mechanisms and corresponding radar signatures indicative of downdraft presence.

Downdraft forcing mechanisms	Radar signatures
Evaporational cooling	Radial convergence below cloud base, particularly when Z_b decreases significantly towards the ground. Radial convergence above cloud base, particularly when associated with a Z_b notch and/or a very dry environmental layer.
Melting cooling	Radial convergence just below the 0°C level.
Precipitation drag	Radial convergence within a descending reflectivity core > 50 dBZ _e .
Vertical pressure gradients	Azimuthal radial velocity couplet indicative of rotation, especially when vorticity increases with decreasing height.

X

TO BE DISCUSSED LATER

Roberts and Wilson 1989

31 May 1994 © H. Bluestein

- EVAPORATION OF PRECIPITATION
DRIVES NEGATIVE BUOYANCY –
DRY MICROBURST

- KICKING UP DUST – MICROBURST: DANGEROUS
FOR LANDING AIRCRAFT

AIR PARCEL
FOLLOWS
MOIST
ADIABAT DOWN
UNTIL ALL
PRECIP. HAS
EVAPORATED;
THEN AIR
PARCEL
FOLLOWS
DRY ADIABAT

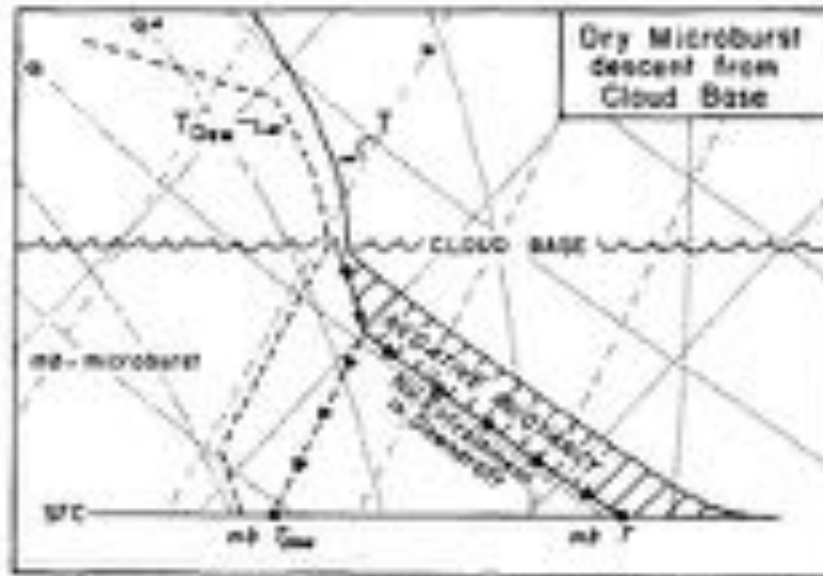


FIG. 10. Model of the thermodynamic descent of a dry microburst from cloud base. Surface temperature and dew-point temperature within the microburst are determined from PAM data. No entrainment into the downdraft is assumed.

Wakimoto 1985

- WATER LOADING DRIVES NEGATIVE BUOYANCY – WET MICROBURST

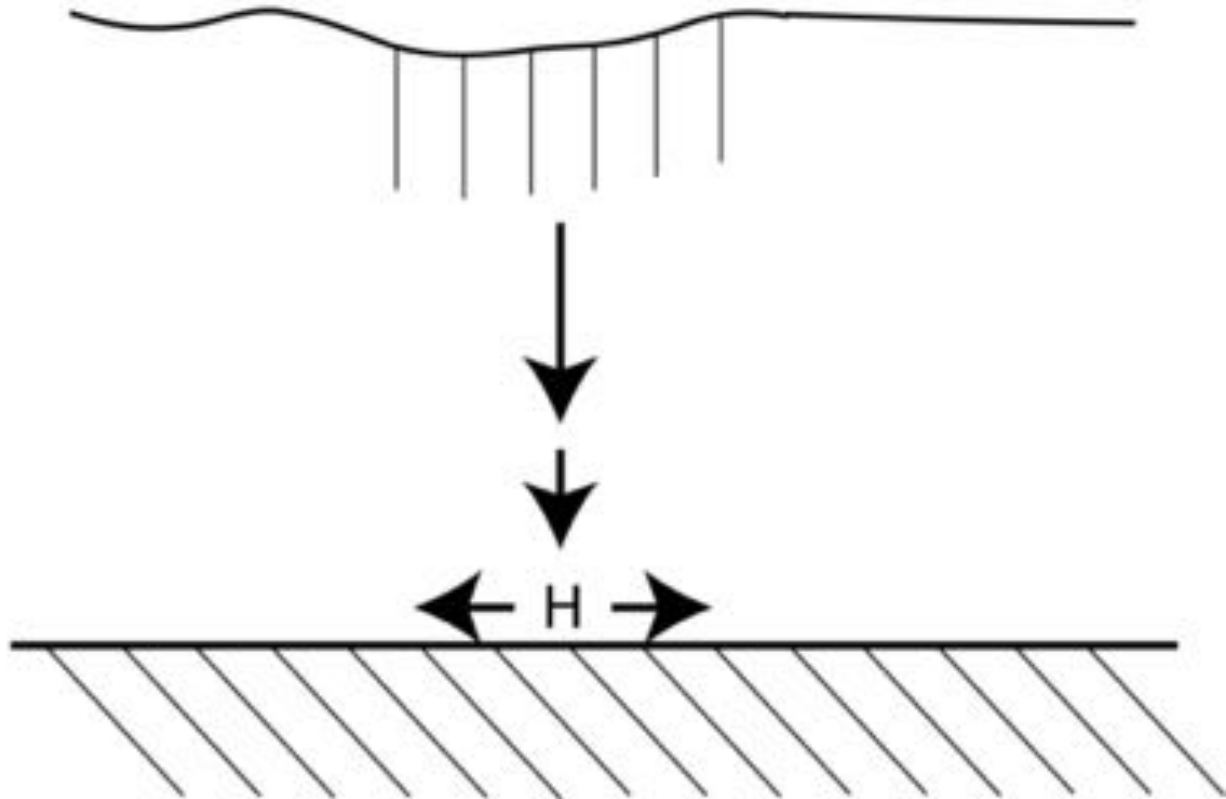
26 July 1978 © H. Bluestein

WET MICROBURST OVER OKLAHOMA CITY

An aerial photograph showing a large, dark, rectangular structure, possibly a dam or a large building, situated in a body of water. The structure is dark and appears to be a solid mass. The water around it is a deep blue color. The sky is dark and overcast. The overall scene is somewhat somber and industrial.

27 Aug. 1993 © H. Bluestein

CLOUD



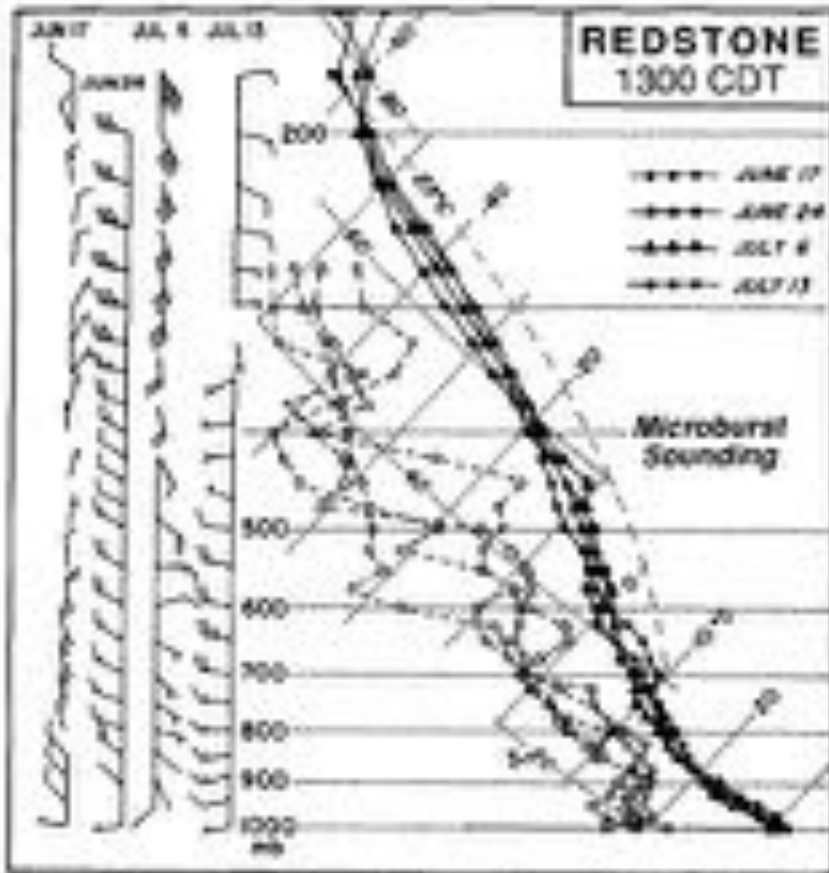


FIG. 8. Data from rawinsondes launched at 1300 CDT for 17, 24 June and 6, 13 July. As in Fig. 7, the soundings are centered on 17 June (unshifted). The other temperature profiles were shifted by: -0.5°C (24 June), -0.3°C (6 July), and -1.1°C (13 July). The moisture profiles were shifted by: -4.1°C (24 June), -2.0°C (6 July), and -3.4°C (13 July).

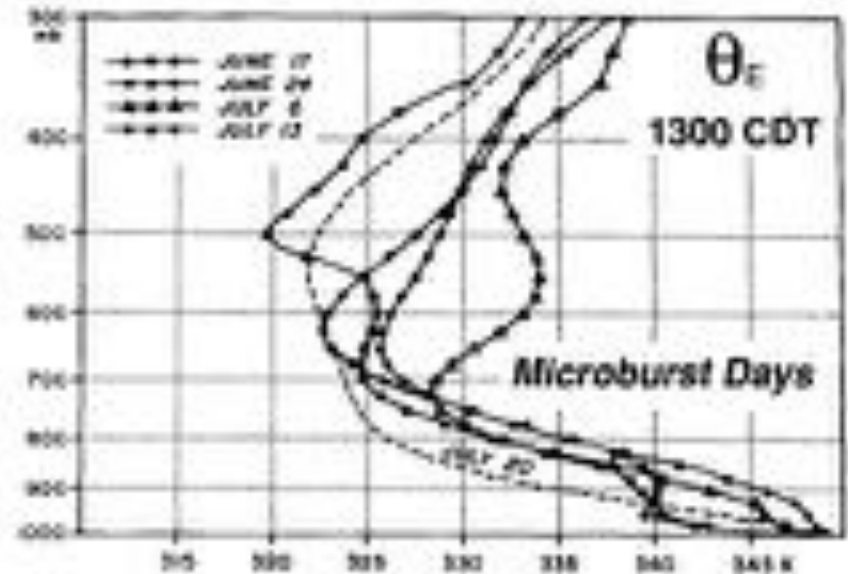


FIG. 10. Same as Fig. 9 but for 1300 CDT. The profiles have been shifted by: -6.0 K (24 June), 0.2 K (6 July), -3.2 K (13 July), and -8.6 K (20 July).

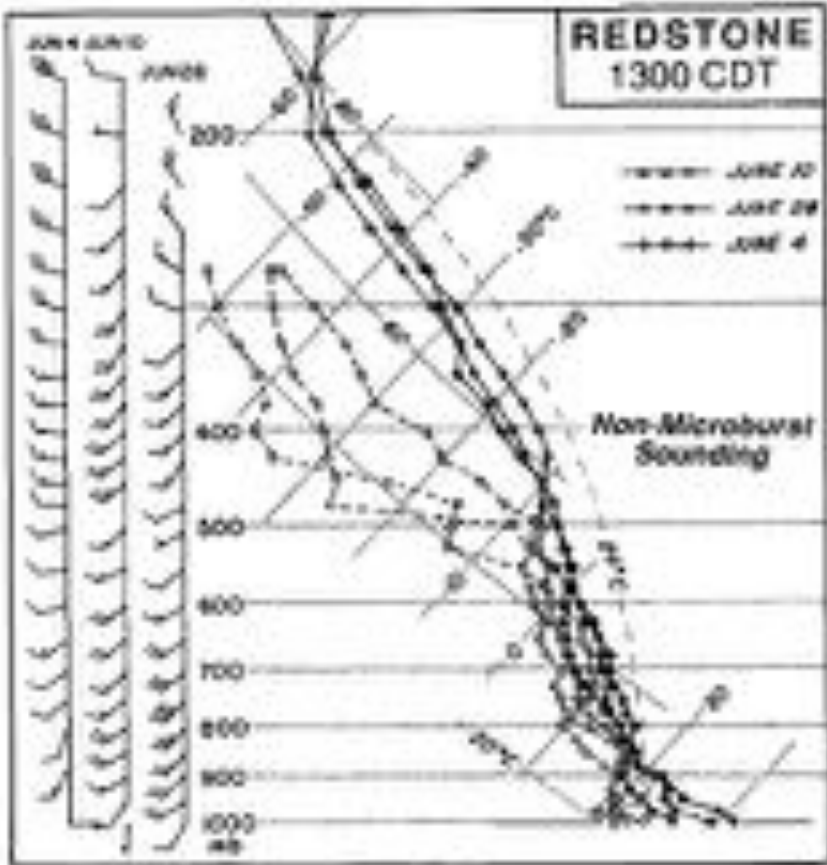


FIG. 13. Rawinsondes launched at 1300 CDT for the null days. The soundings are centered on 10 June (unshifted). The other temperature profiles have been shifted by: 3.2°C (4 June) and 0.2°C (28 June). The moisture profiles were shifted by: 3.0°C (4 June) and 2.1°C (28 June).

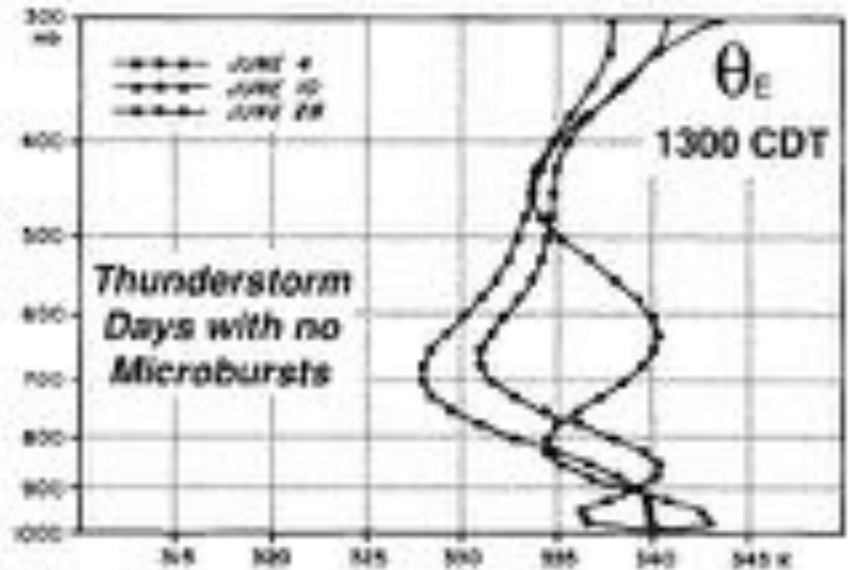


FIG. 15. Same as Fig. 14 but for 1300 CDT (including 4 June). The profiles have been shifted by: 3.4 K (4 June) and -5.6 K (10 June).

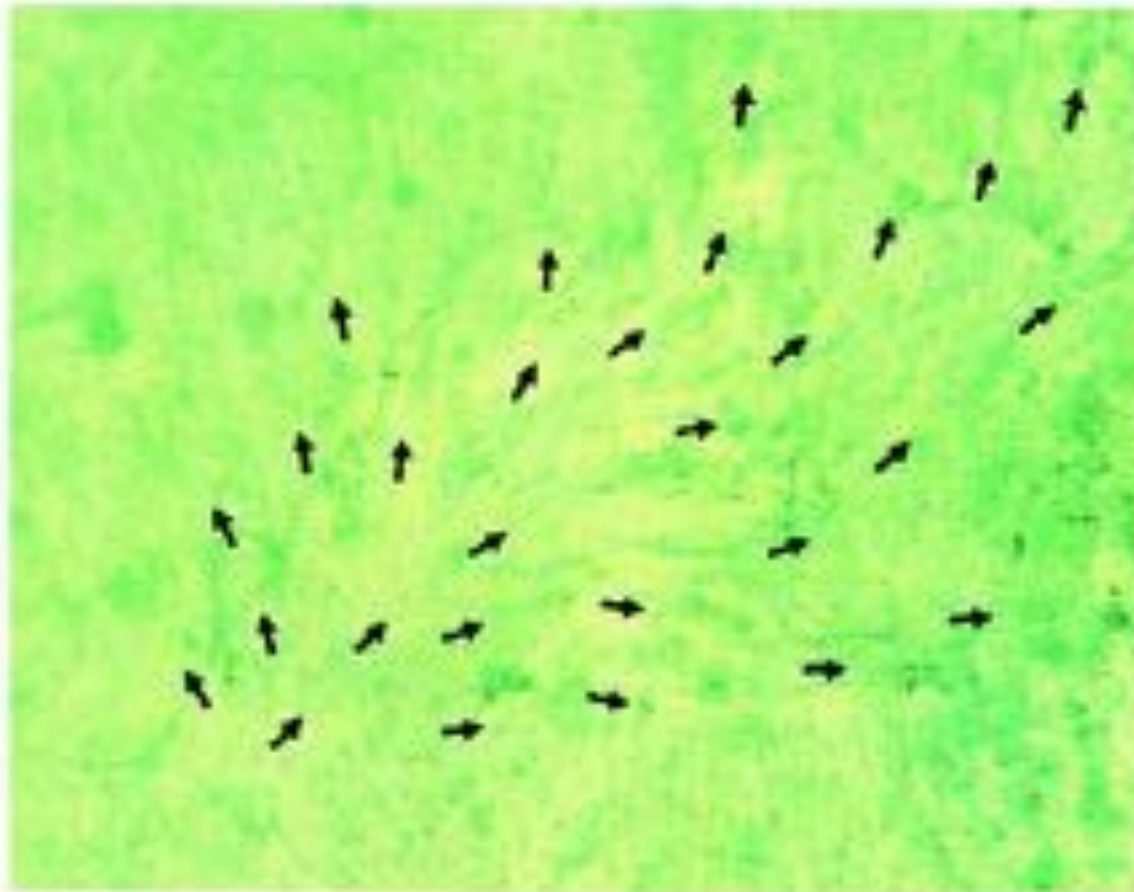


FIG. 1. Starburst pattern of uprooted trees associated with a downburst photographed by Fujita near Beckley, WV, following the superoutbreak of tornadoes on 3-4 Apr 1973. It was such damage patterns that gave Fujita the ideas for the existence of downbursts. [From Fujita (1985)]

“STARBURST PATTERN” OF GROUND DAMAGE

- DUAL-DOPPLER ANALYSIS OF A MICROBURST AT THE GROUND

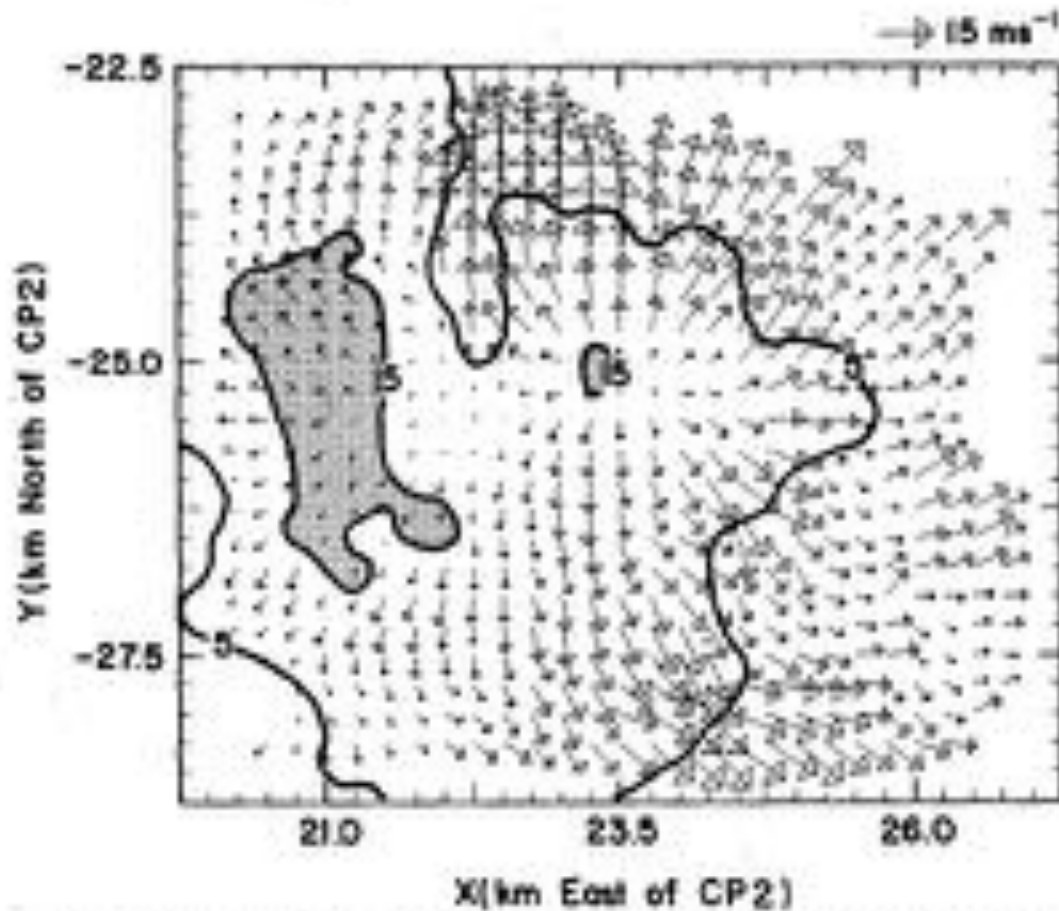


FIG. 2. Horizontal winds and reflectivity contours at lowest-level analysis (~ 50 m) for microburst A at 1445 MDT on 14 July 1982. Wind arrows are scaled as shown in upper right. Reflectivity contours in dBZ as shown.

- POLARIMETRIC RADAR SIGNATURE OF MICROBURST

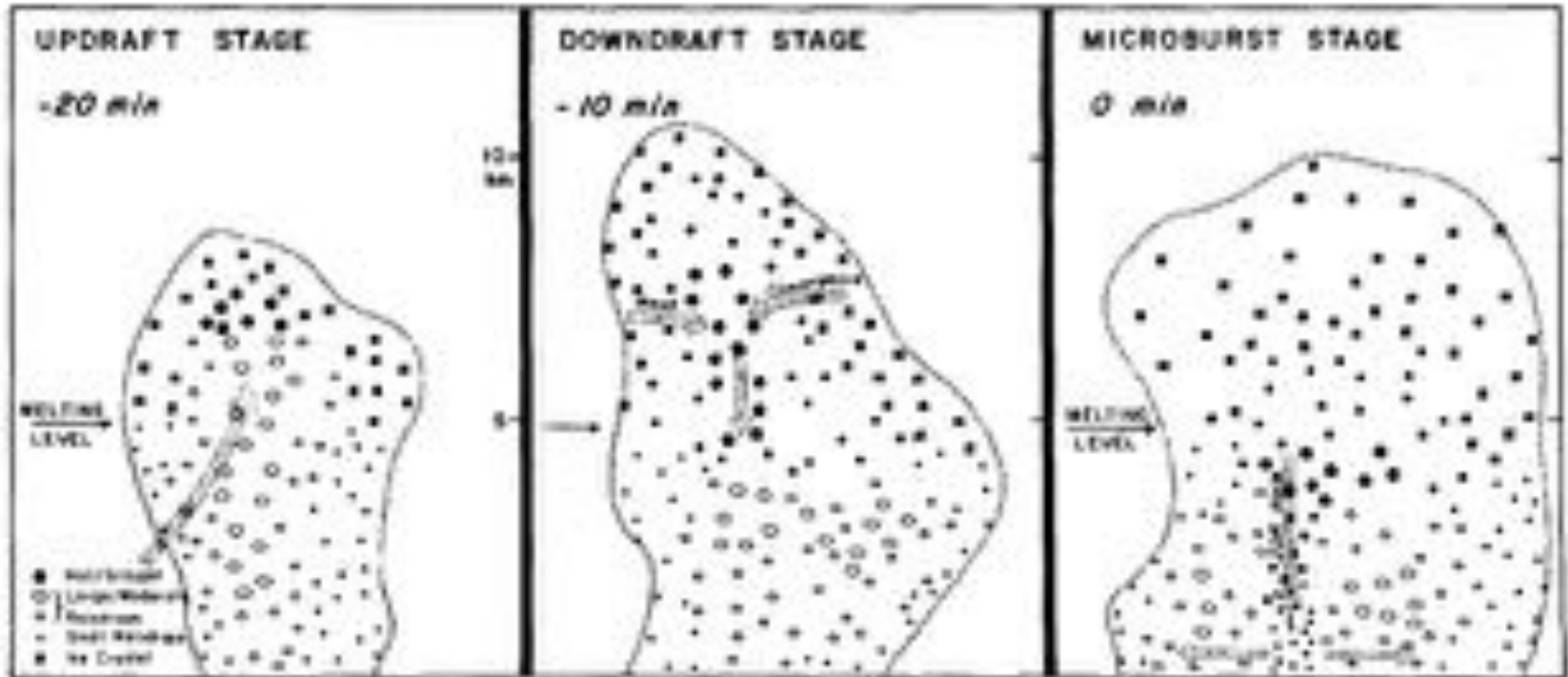
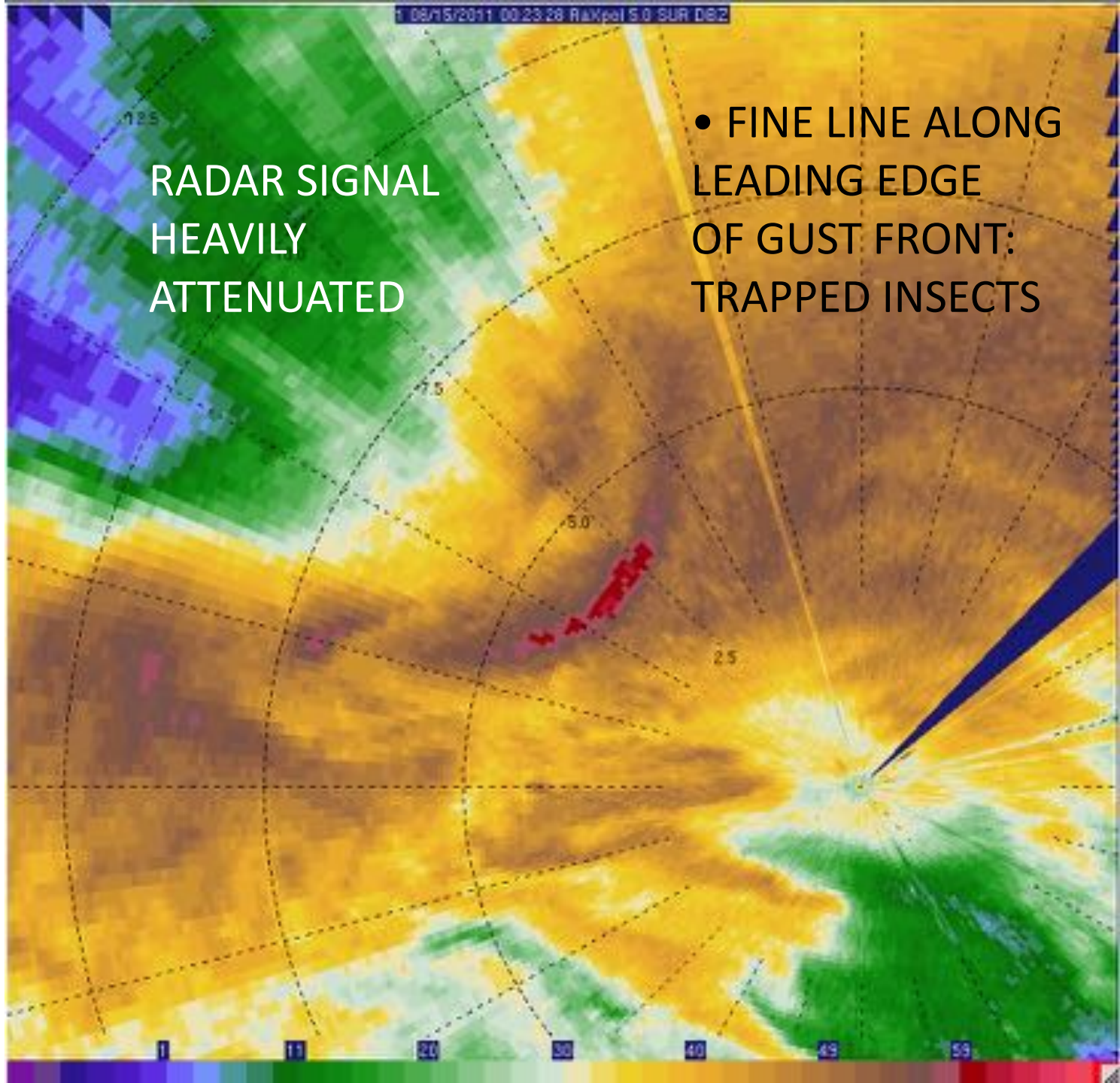


FIG. 11. Schematic model of the microphysical evolution of the 20 July storm.

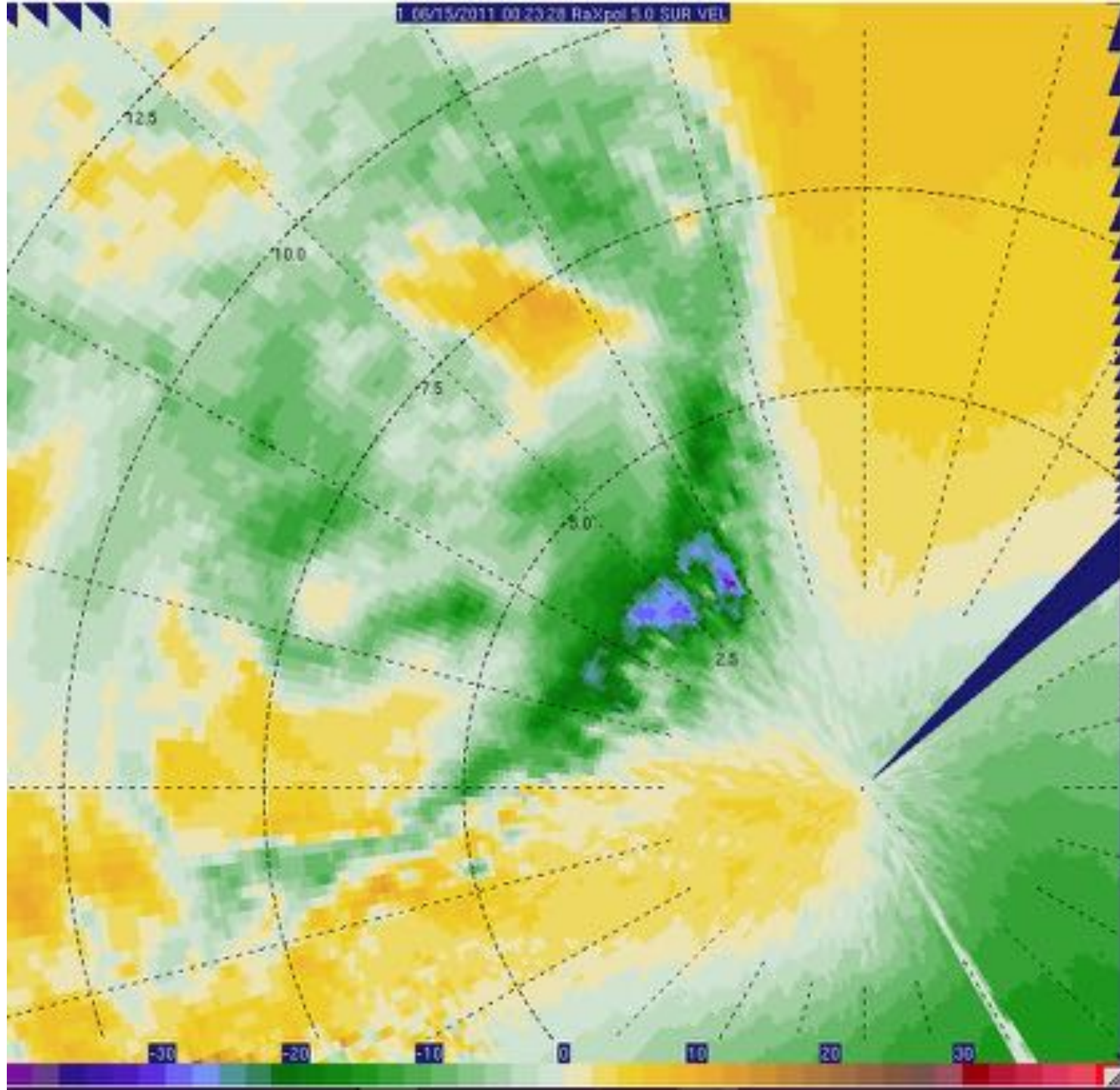
Wakimoto and Bringi 1988 Z_{DR} HOLE

14 June 2011
RaXPol

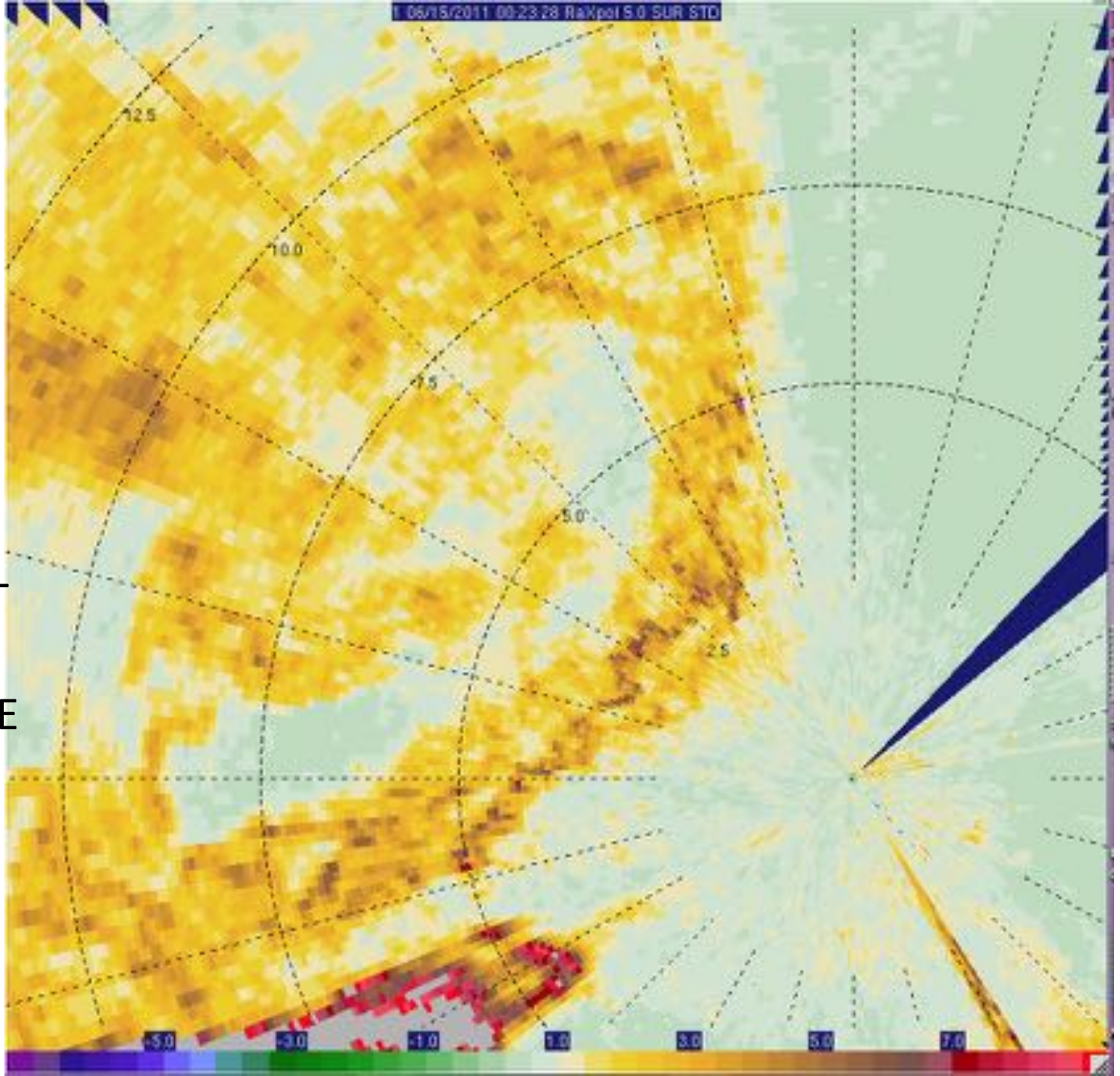
- Damaging microburst in Norman, OK

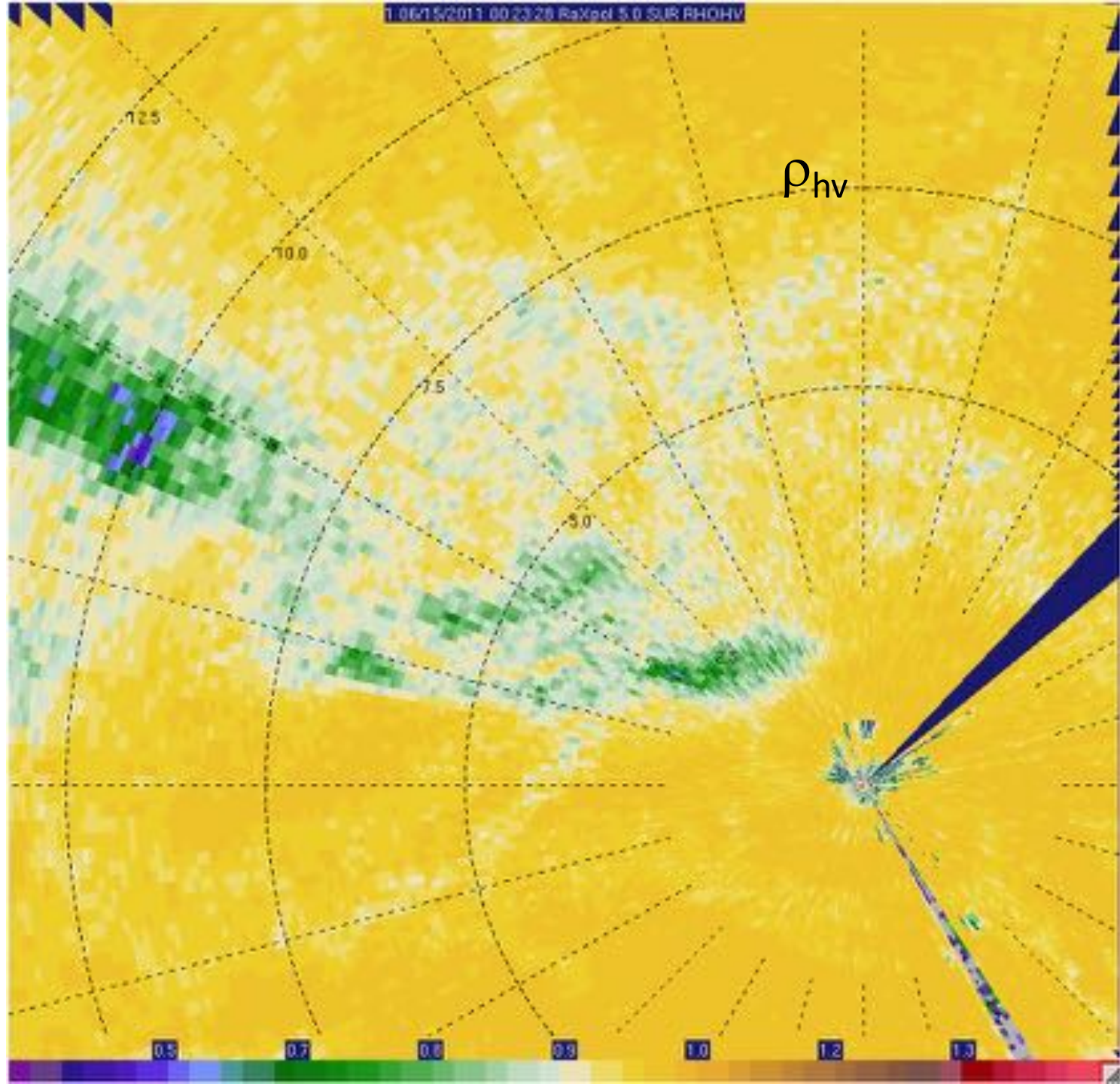


- DOPPLER VELOCITY SHOWING BOWING EDGE OF GUST FRONT



- HIGH SPECTRUM WIDTH ALONG LEADING EDGE OF GUST FRONT - STRONG TURBULENCE

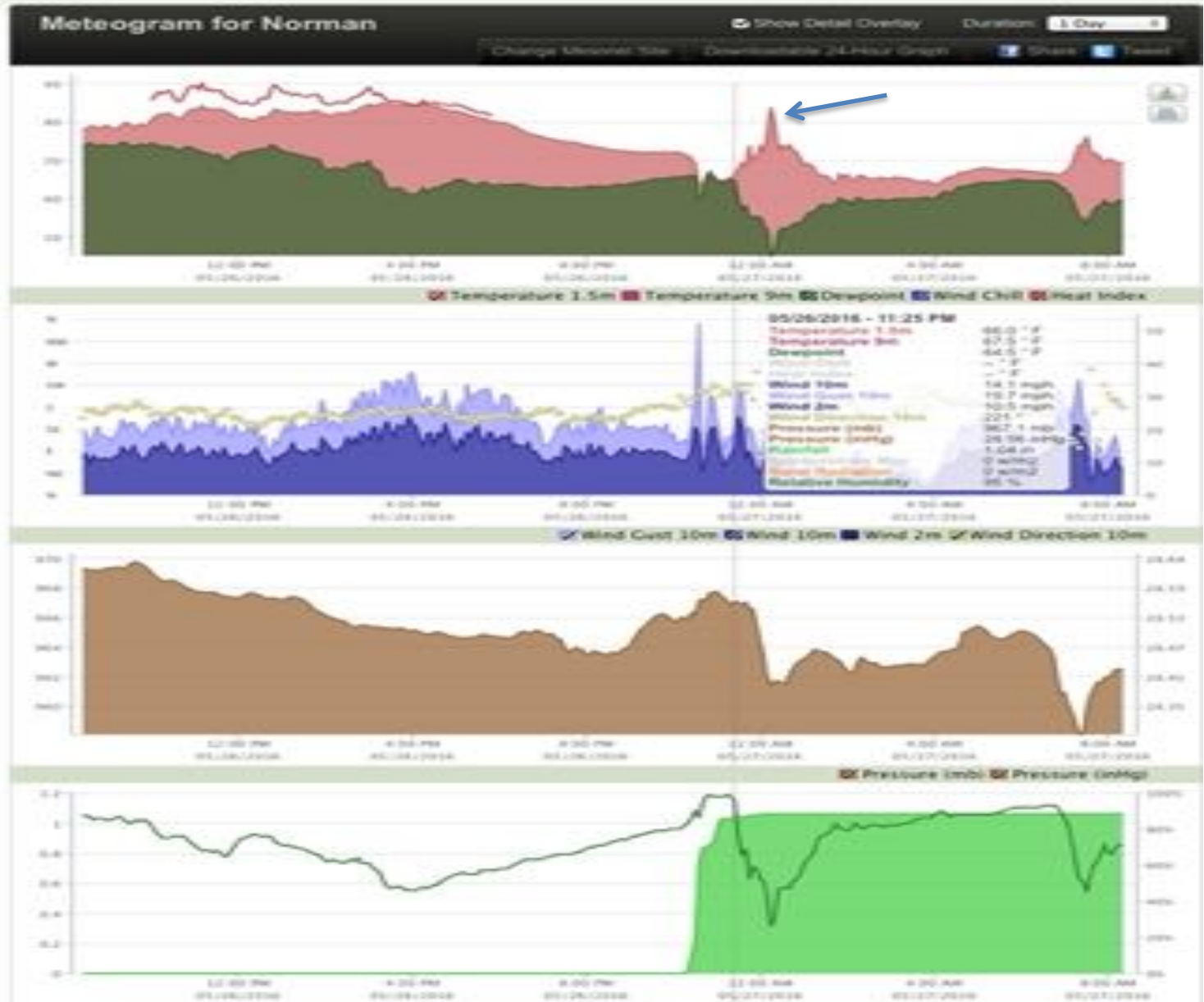




- LOW ρ_{hv}

DUST, HAIL
(IF Z HIGH)

- Local Weather 3
- Radar 3
- Air Temperature 3
- Rainfall 3
- Wind 3
- Dewpoint & Humidity 3
- Pressure 3
- Solar Radiation & Satellite 3
- Soil Temperature 3
- Soil Moisture 3
- Ground Water 3
- Station Photo 3
- Station Meteograms 3
- Past Data & Files 3
- Advisories 3
- Upper Air 3



• HEAT BURST

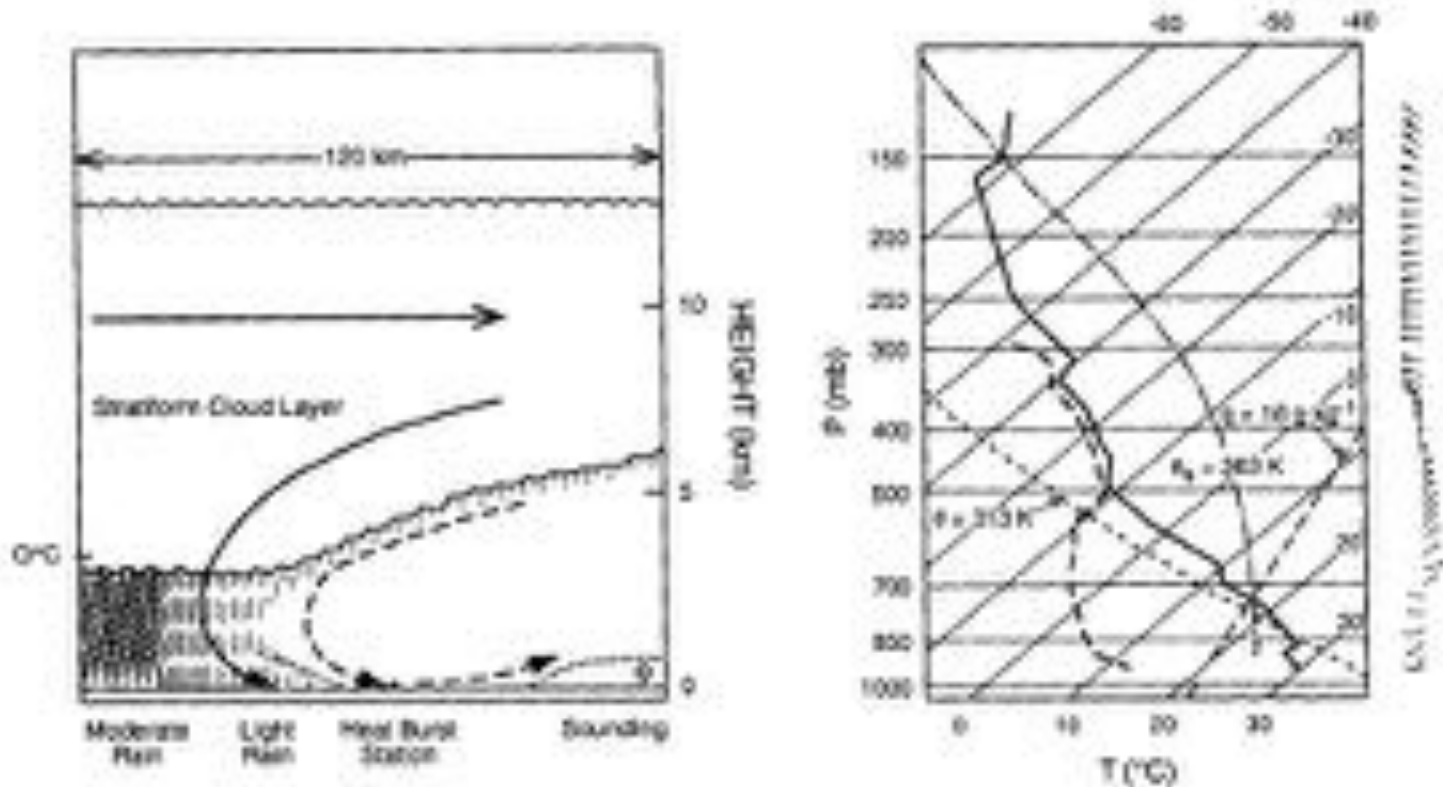
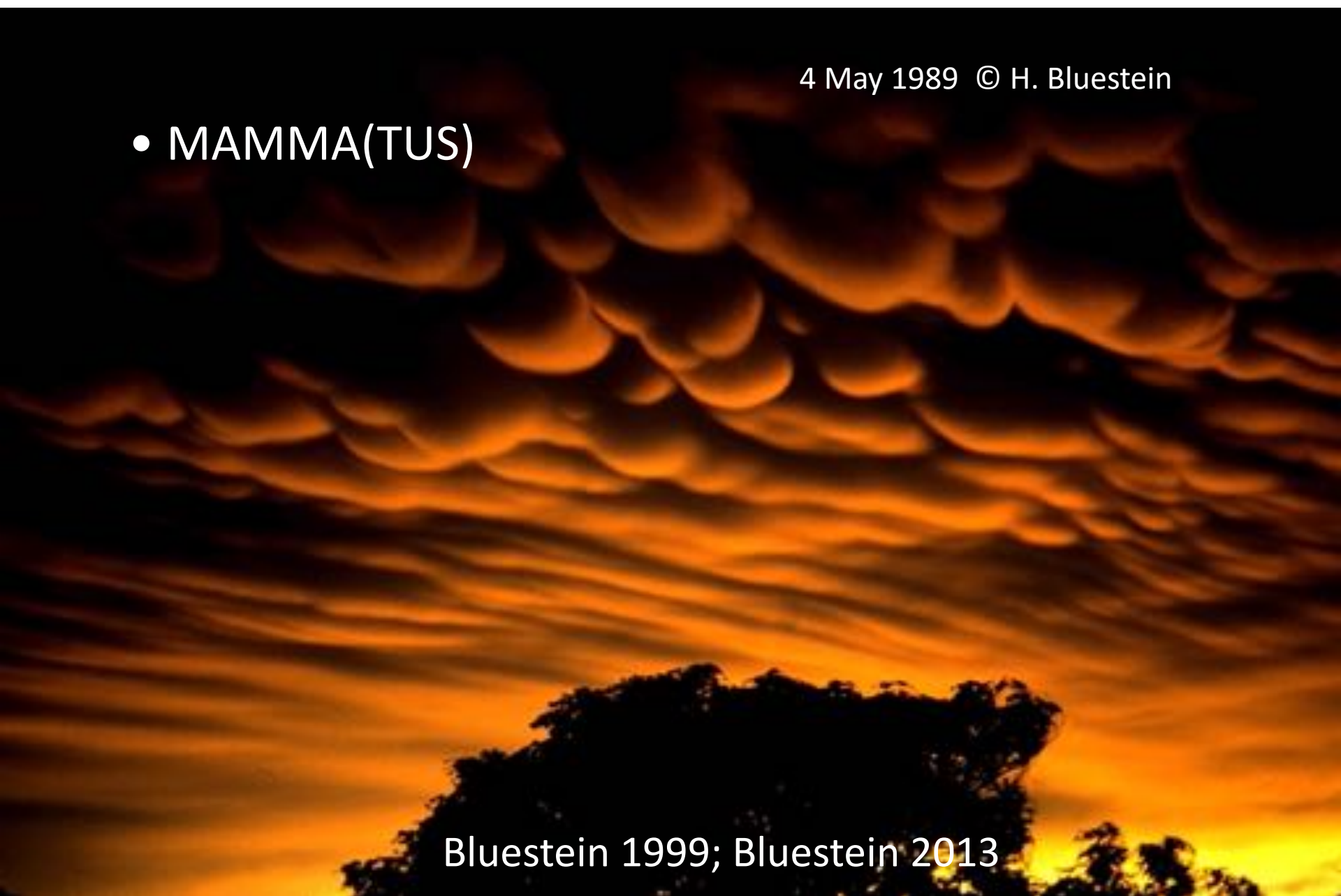


FIG. 15. Conceptual model of a heat burst as a deformation of a shallow, cool, moist stable layer at the surface by a descending circulation of warm, dry air from aloft. Solid arrows represent winds verified by dual-Doppler data. The dashed arrow represents proposed heat burst wind. Dotted lines represent the upper boundary of the moist stable layer. Heat burst conceptual sounding adapted from the 0440 UTC RSE sounding. The locations of the sounding and surface station are denoted.

4 May 1989 © H. Bluestein

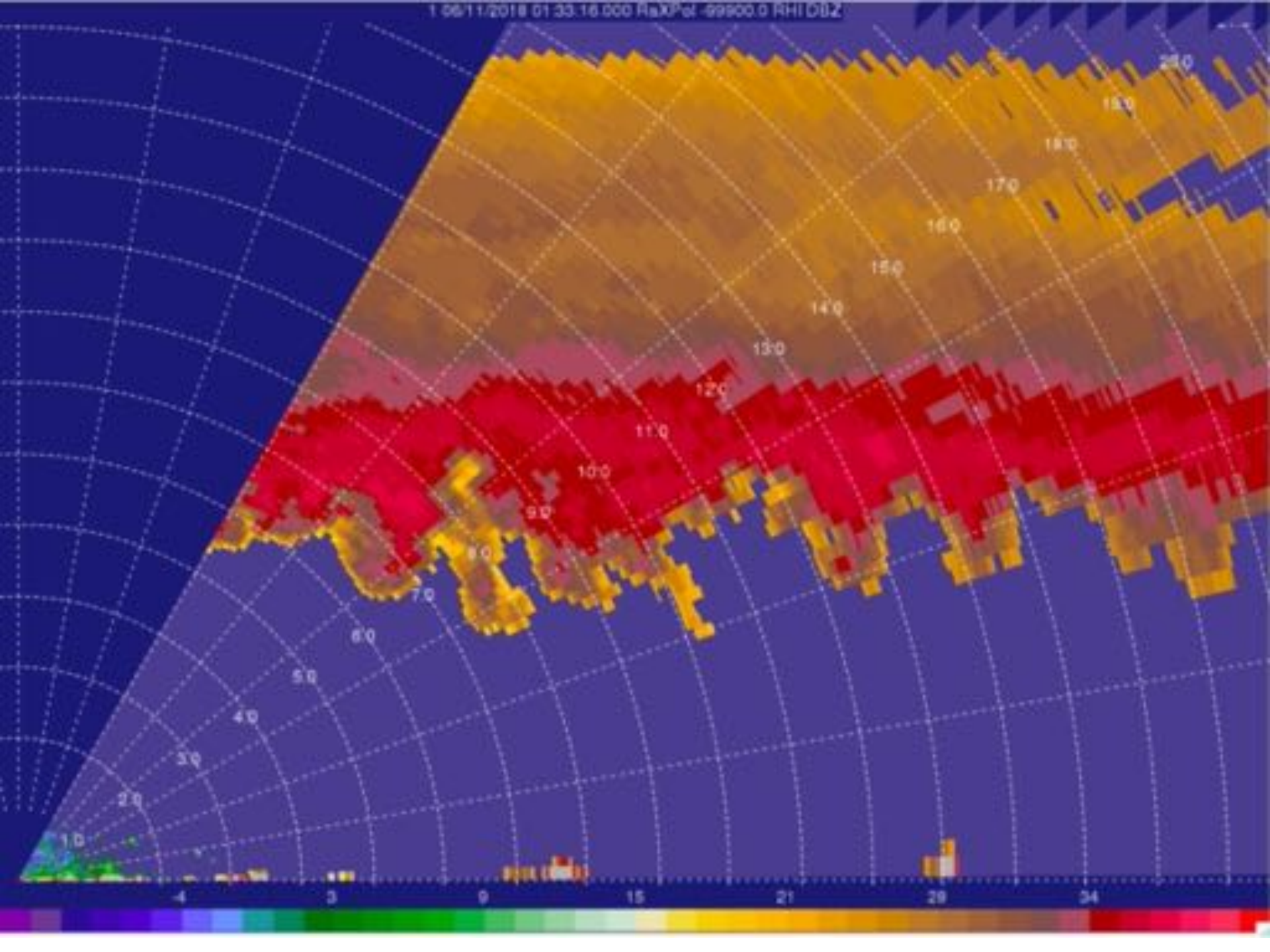
- MAMMA(TUS)

Bluestein 1999; Bluestein 2013

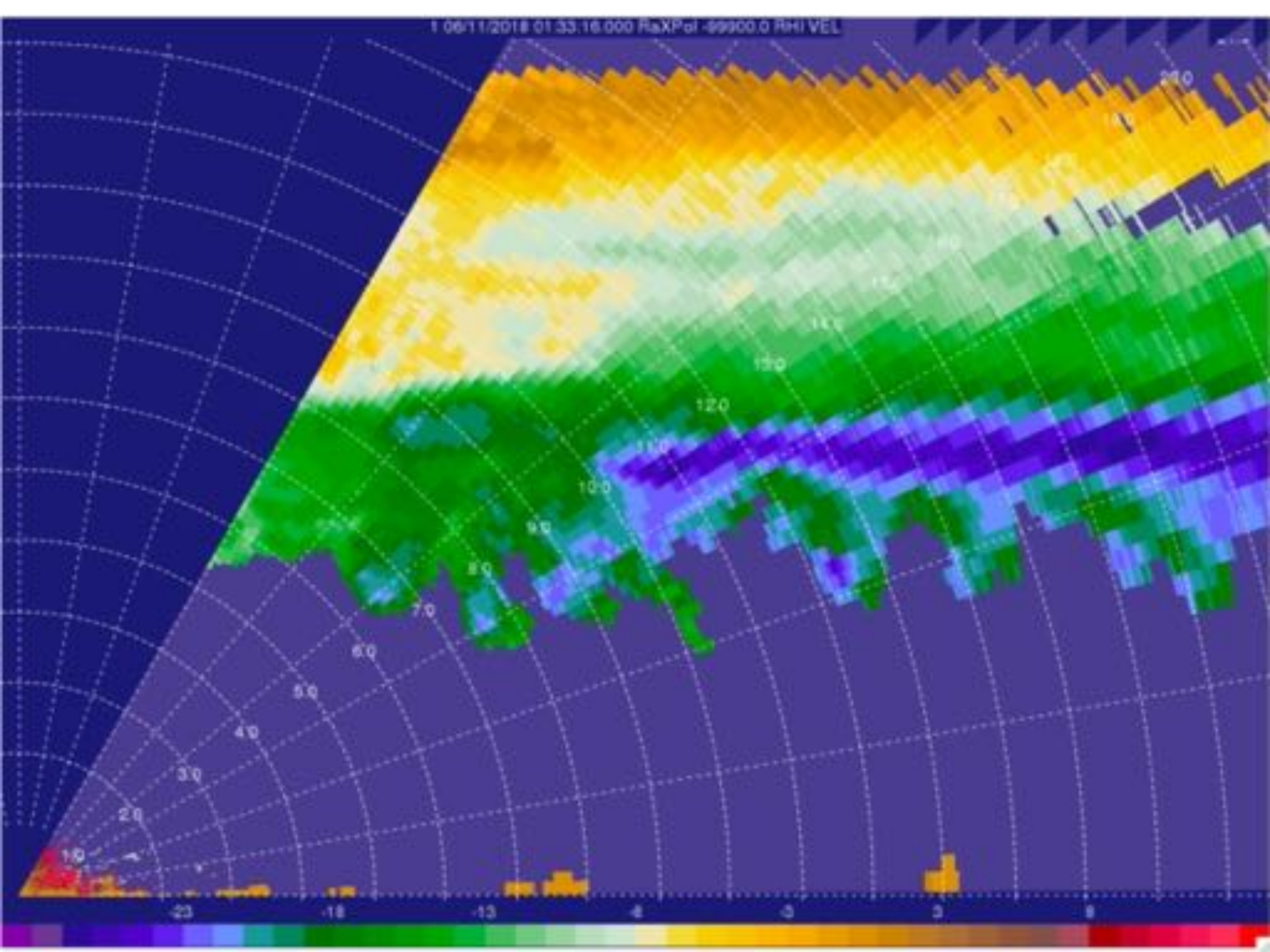


26 May 1997
© H. Bluestein





1 06/11/2018 01:33:16.000 RbXPol -99900.0 RHI VEL



FLIGHT THROUGH MAMMA

M
a
r

- Z HIGH WHEN DOPPLER VELOCITY (DOWNDRAFTS) $W < 0$

n
e
r
1
9
9
5

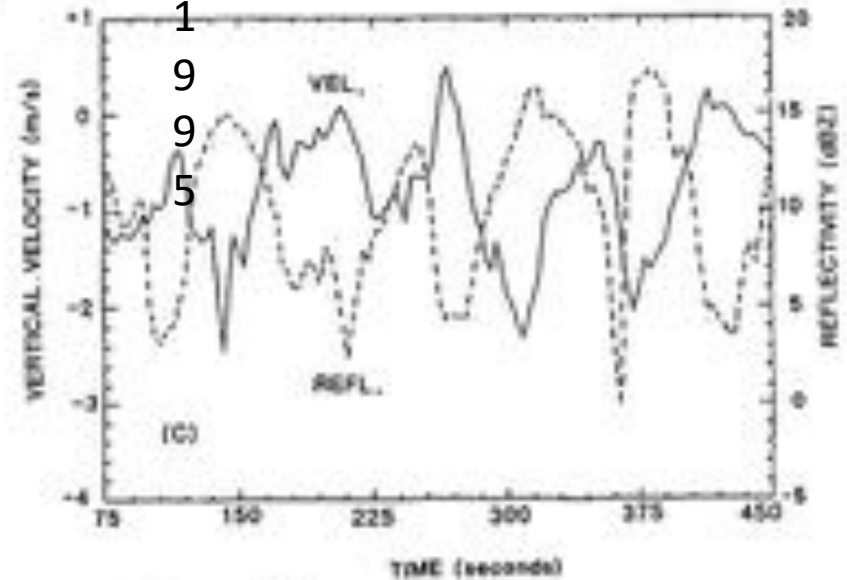
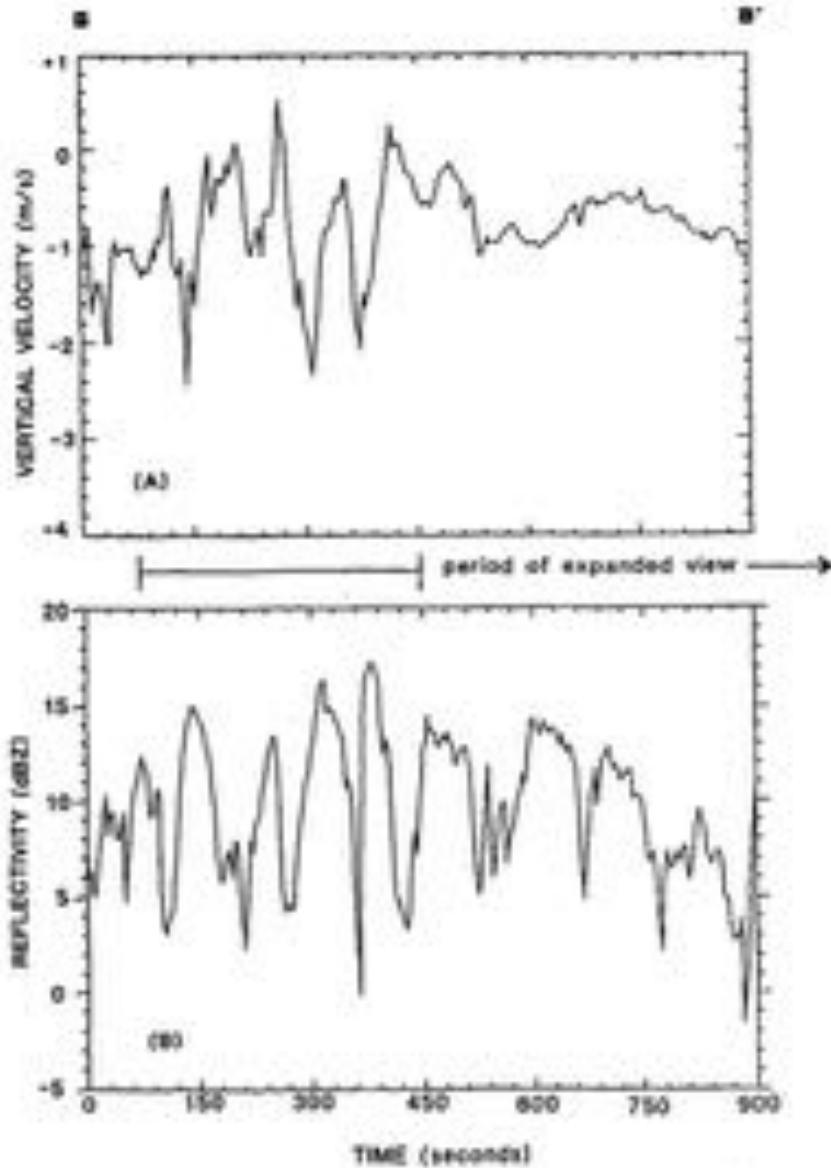


FIG. 4. Time series of data along the BB' cross section near the bottom of the mammatus elements, including (a) vertical velocity, (b) reflectivity, and (c) an expanded view of both.

W

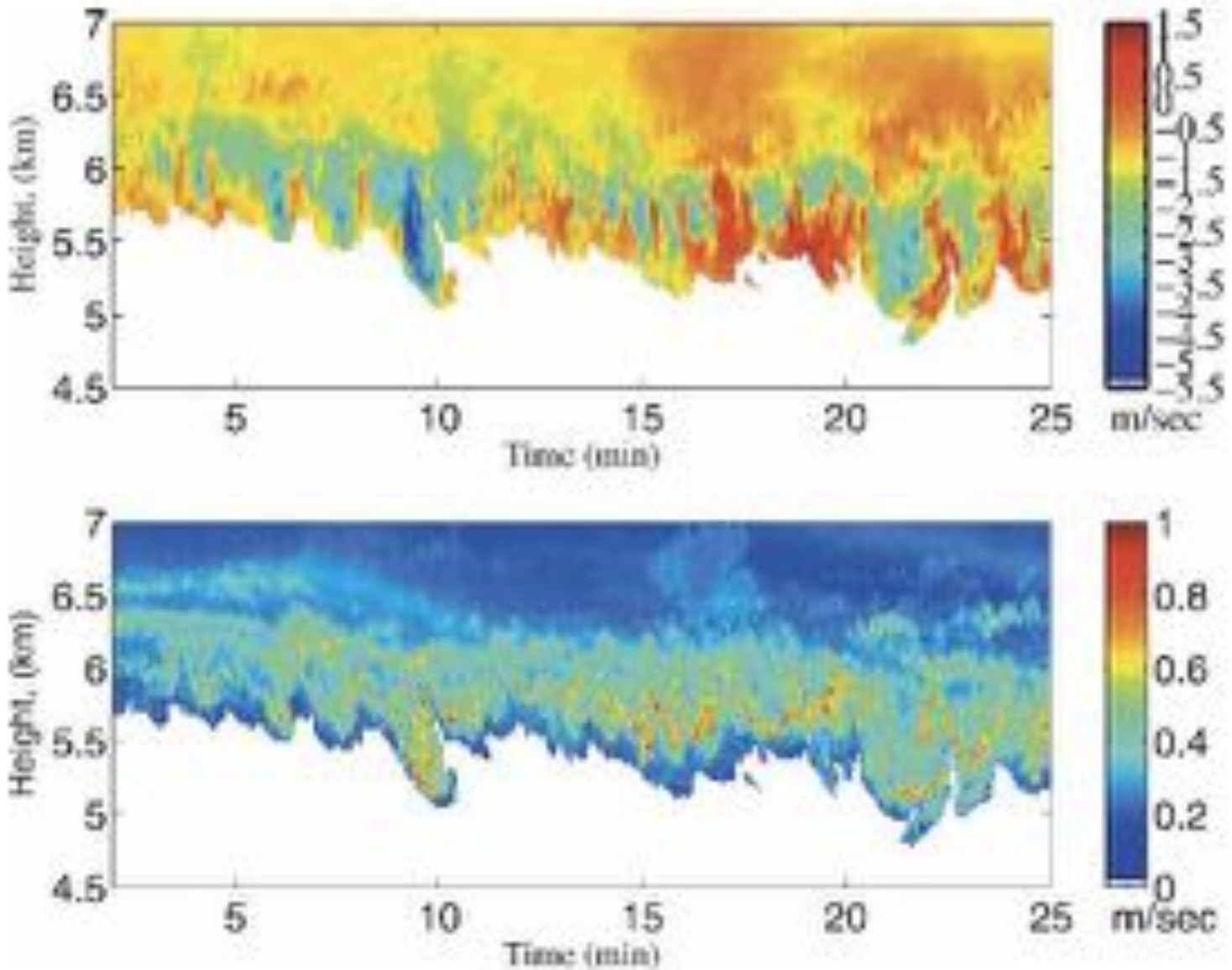


FIG. 2. High-resolution observations of (top) zanzanas mean Doppler velocity and (bottom) Doppler spectrum width from the UMDCR.

Kanak et al.
2008

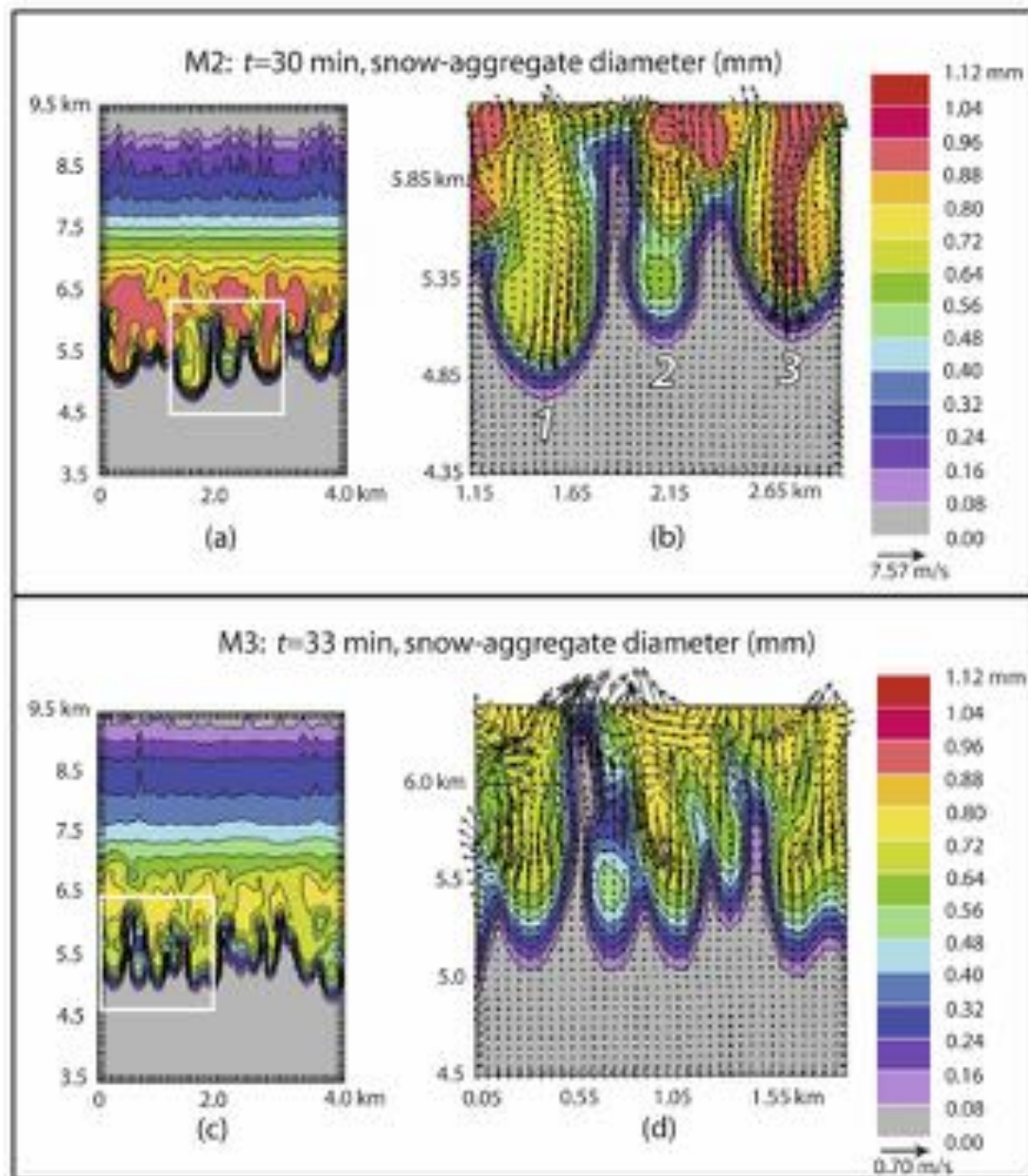
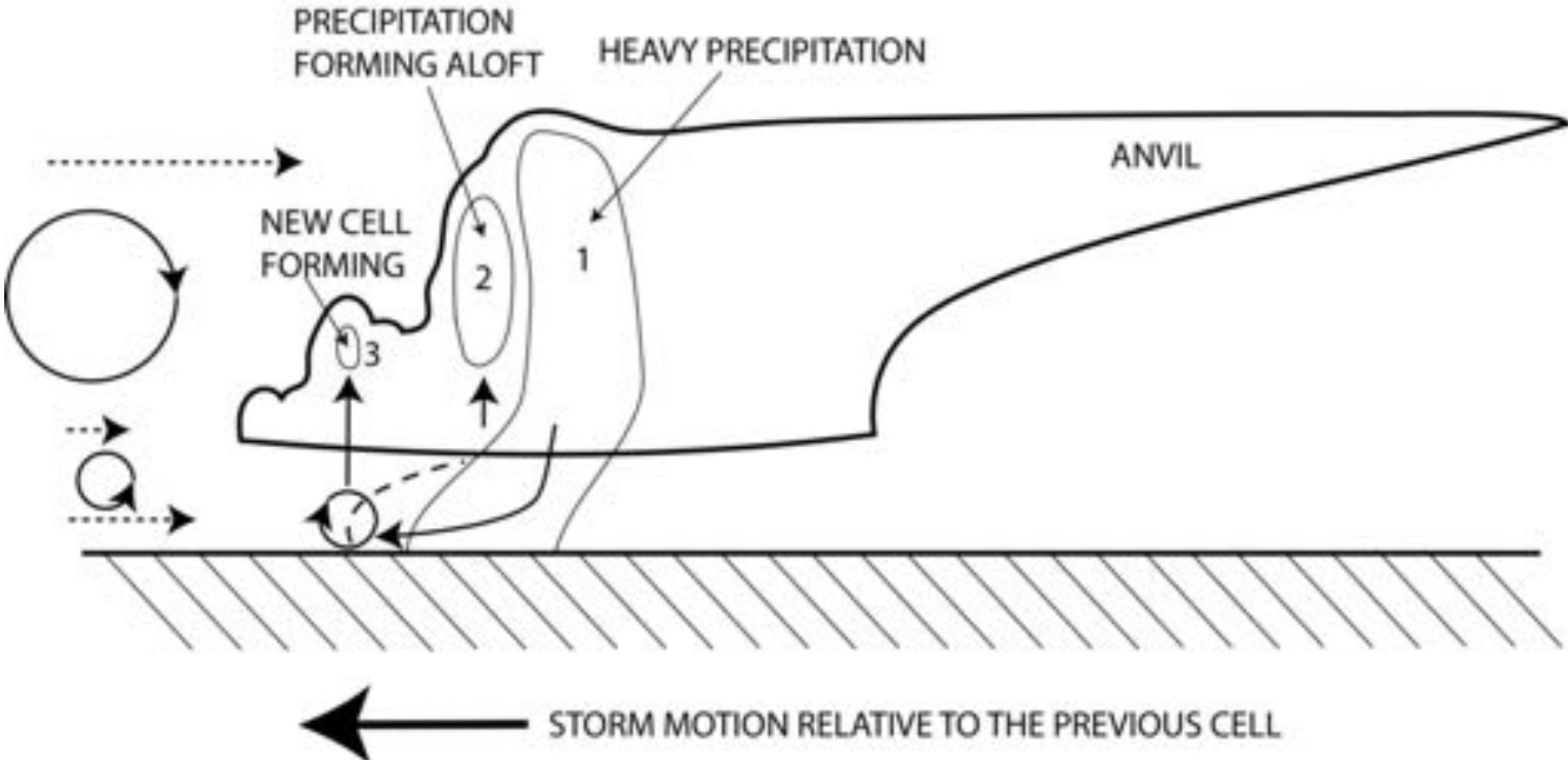
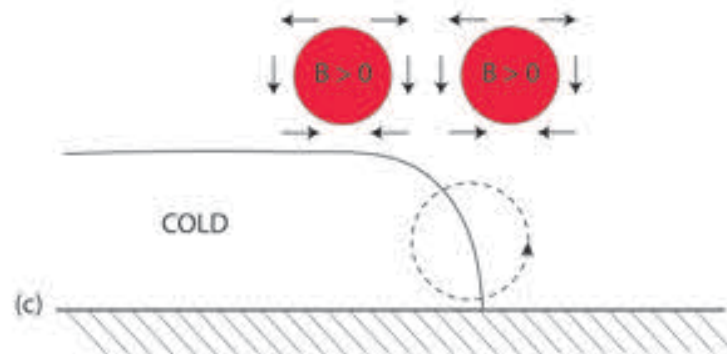
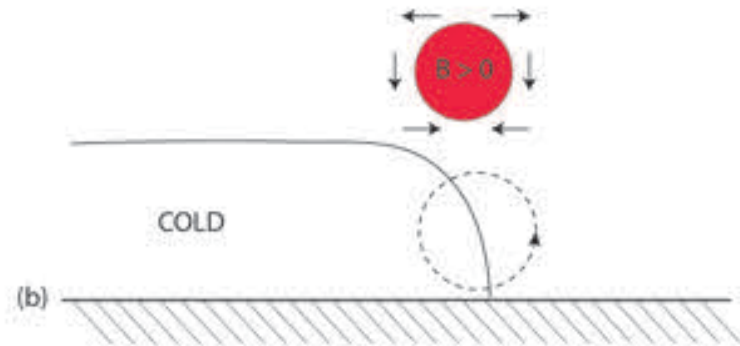
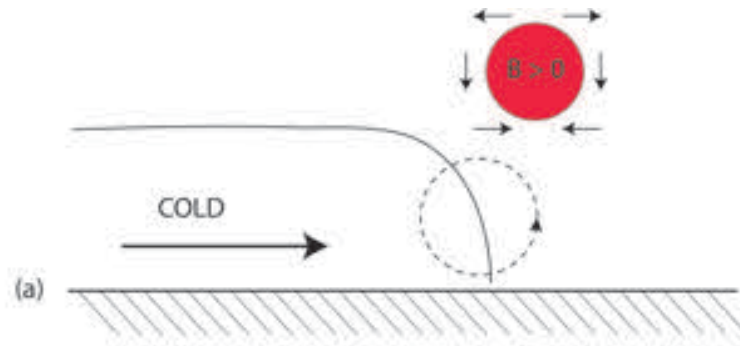


FIG. 3. Vertical cross sections of snow aggregate diameter (mm, color contours). (a) M2: whole domain at $t = 30$ min and $y = 75$ m. (b) M2: inset with velocity vectors. White box in (a) indicates inset in (b). The longest vector corresponds to a wind speed of 7.57 m s^{-1} . Large white numbers represent individual mammatus lobes described in text. (c) M3: whole domain at $t = 33$ min and $y = 1625$ m. (d) M3: inset with velocity vectors. White box in (c) indicates inset in (d). The longest vector corresponds to a wind speed of 0.70 m s^{-1} .

ANATOMY OF A MULTICELL CONVECTIVE STORM





SUMMARY:

- BUOYANCY – UPDRAFTS AND DOWNDRAFTS
- GUST FRONTS – DOWNDRAFTS HIT THE GROUND
- ORDINARY-CELL CONVECTIVE STORMS – UPDRAFT, FOLLOWED BY DOWNDRAFT WHERE UPDRAFT USED TO BE: “THAT’S ALL FOLKS!”

UPDRAFTS GONE WILD: LARGE HAIL

GUST FRONTS GONE WILD: MICROBURSTS

DOWNDRAFTS GONE EXOTIC: HEAT BURSTS

DOWNDRAFTS ALOFT GONE EXOTIC: MAMMA

*NEXT: GUST FRONTS AND BUOYANCY GONE WILD!
VERTICAL SHEAR ADDED...*